Ti 4

REPORT NO. FRA-OR&D-76-271 PB

STUDY OF FRICTION AND CREEP BETWEEN STEEL WHEELS AND RAIL

DEPARTMENT OF TRANSPORTATION ★ UNITED STATES OF AMERICA ★

JULY 1976

FINAL REPORT

Prepared for

U. S. DEPARTMENT OF TRANSPORTATION
FEDERAL RAILROAD ADMINISTRATION
Office of Research and Development
Washington, D.C. 20590

TECHNICAL REPORT STANDARD TITLE PAGE

1. Report No.	2. Government Accession No.	3. Recipient's Catalog No.
FRA/OR&D-76/271	-	-

4. Title and Subtitle	5. Report Date / 6. Performing Organization Code
Study of Friction and Creep Between Steel Wheels and Rail	July 1976 / -
7. Author(s)	**8. Performing Organization Report No.**
C. Sciammarella, M. Press, S. Kumar B. Seth, S. Nailescu and S. Kalpakjian	IIT-TRANS-76-2
9. Performing Organization Name and Address	**10. Work Unit No.** / **11. Contract or Grant No.**
Illinois Institute of Technology Department of Mechanics, Mechanical and Aerospace Engineering Chicago, Illinois 60616	- / DOT-OS-40103
12. Sponsoring Agency Name and Address	**13. Type of Report and Period Covered** / **14. Sponsoring Agency Code**
1. U.S. Department of Transportation 2. General Motors, Electro-Motive Division 3. Association of American Railroads	Interim Technical Report / -

15. Supplementary Notes

This study has, also, partially been supported by the Illinois Institute of Technology Chicago, Illinois 60616

16. Abstract

A systematic experimental, parametric and similitude investigation of the friction and creep behavior of a steel wheel rolling on a steel rail is given. Laboratory investigation was performed on the 1/5th scale experimental GM-IIT Wheel Rail Simulation Testing Facility reported on earlier. Investigation of the size and area of contact between the two wheels at different stages of surface wear shows that the initially elliptical (near Hertzian) area of contact changes fast into a near rectangular shape with a several-fold increase, depending on the load and the duration of testing and wear. It was found that Kalkers Theory fits the nondimensionalized data well, when wheel surfaces are near perfectly smooth. The product of actual contact area and creep is always constant for a given normal load and friction coefficient regardless of the surface roughness and wear time ($\lesssim$ 5 hrs.). This constancy law was derived on the basis of experimental data. It has been shown here that for the elastic and smooth surfaces the Carter-Poritsky theory also predicts the product of creep and theoretical area of contact as constant for a given load and operating friction coefficient. Generalized expressions for the interrelationship of friction coefficient, creep, actual area of contact, normal load and shear modulus have been established on the basis of experimental data. Recommendations for future design improvements have been made on the basis of these relations.

17. Key Words	18. Distribution Statement
Friction, Creep, Adhesion, Traction, Contact Zone	Document is available to the public through the National Technical Information Service, Springfield, Virginia 22161

19. Security Classif. (of this report)	20. Security Classif. (of this page)	21. No. of Pages	22. Price
Unclassified	Unclassified	108	-

Form DOT F 1700.7 (8-69)

ACKNOWLEDGMENTS

This research work was sponsored by the U.S. Department of Transportation, the General Motors Electro-Motive Division, the Association of American Railroads and the Illinois Institute of Technology under Contract No. DOT-OS-40103. Their support of this study is thankfully acknowledged.

We are very thankful to the Engineering staff of the Electro-Motive Division of General Motors and especially to Messrs. Henry Marta, Ken Mels and Gordon Itami for providing technical assistance toward this study. Sincere thanks are extended to Mr. R. Gandhi for providing enormous assistance during experimentation. Our gratitude is due to Dr. Brij B. Seth, for his assistance and guidance during experimentation and to Mr. Gene Ginani and Mr. Jerry Busiel for their technical assistance.

We wish to express our true appreciation and most sincere thanks to Mrs. Anita Ter Haar and Mrs. Carol Timkovich, and Miss Pauline Guadagno for their patient and careful typing of this work.

S. Kumar - Project Director
C. Sciammarella - Task Leader
and other authors

TABLE OF CONTENTS

LIST OF FIGURES

LIST OF FIGURES - Cont'd.

LIST OF FIGURES - Cont'd.

LIST OF TABLES

I

INTRODUCTION

With the introduction of new-powered engines, one of the main objectives of the railroad industry is to improve the maximum available tractive effort and to haul loads at higher speeds. Several methods have been suggested over the period of the past few years, whereby this objective can be achieved. Increasing the number of wheels, increasing the load per wheel, sanding of the track and cleaning the track by plasma torch are some of the most recommended methods of achieving improved adhesion. Operation of locomotives using high adhesion coefficients has generally shown simultaneous increase in wear rates of the wheel and the rail. Large wear rates are not considered acceptable due to obvious increases of operational costs. It is therefore desirable to have maximum available adhesion between a wheel and the rail without giving up too much in terms of track and wheel wear. This calls for a better understanding of the behavior of friction, creep and wear in the small contact region between the wheel and the rail.

The purpose of this investigation, therefore, is to make a systematic study of friction and creep between steel wheels and rail. It throws light on several important aspects of the problem. A similitude law for smooth and worn surfaces has been established. Variation of area of contact with creep generated with time has also been studied. This understanding of the basic relationship between friction, creep and area of contact is very helpful for a better understanding of adhesion and ways in which to improve it.

The only other experimental work done in this area taking surface roughness into account is by a team at Bolt, Beranek and Newman, Inc.[(3)*] However, their contacting elements were made of aluminum; the area of contact was a rectangle and the change in area of contact with time was not considered. This is not considered to be a true simulation of what exists in actual wheel rail interaction, and the results obtained may not quite reflect the true behavior of a wheel rolling on a rail in our opinion.

* The numbers in parentheses designate references included in the Bibliography.

II.

A BRIEF DISCUSSION OF THE FRICTION CREEP TEST FACILITY

DESIGN AND SIMULATION

The test facility on which this entire study is carried out was originally designed and manufactured at the Electto-motive Division of the General Motors Institute.(1)

In May 1974, this entire 15-ton facility was moved to Illinois Institute of Technology. Several changes were made at this time towards the mechanical as well as the electrical design, operation and control aspects of the rig for performing additional tests with increased accuracy. Thus the facility was significantly improved in its performance and accuracy. The details of the setting up of the facility at I.I.T., its design and control changes and preliminary testing were reported in an earlier I.I.T. Interim Technical Report.(2)

The rig was designed so as to simulate certain road conditions in the laboratory. It essentially consists of one big wheel Fig. 1 [1]* which serves as a rail and one small wheel Fig. 1 [2] which serves as a locomotive wheel. Each of these wheels is powered by a separate motor. The profile of the small wheel has a precalculated radius (see Appendix A), such that when the two wheels are in contact, the area of contact is an ellipse. The ratio of the major axis to the minor axis of this ellipse of contact is the same as that found during actual wheel-rail interaction of G.M. E.M.D. locomotives. This takes care of the geometrical part of the similitude. If the load applied to the contacting wheels is such that the Hertz contact stress(4) developed is equal to the actual Hertz contact stress developed between wheel and rail, the loading part of the similitude is also taken care of. As the effects of

* Numbers in parentheses [ ], written with Fig. 1 refer to components as marked in Fig. 1.

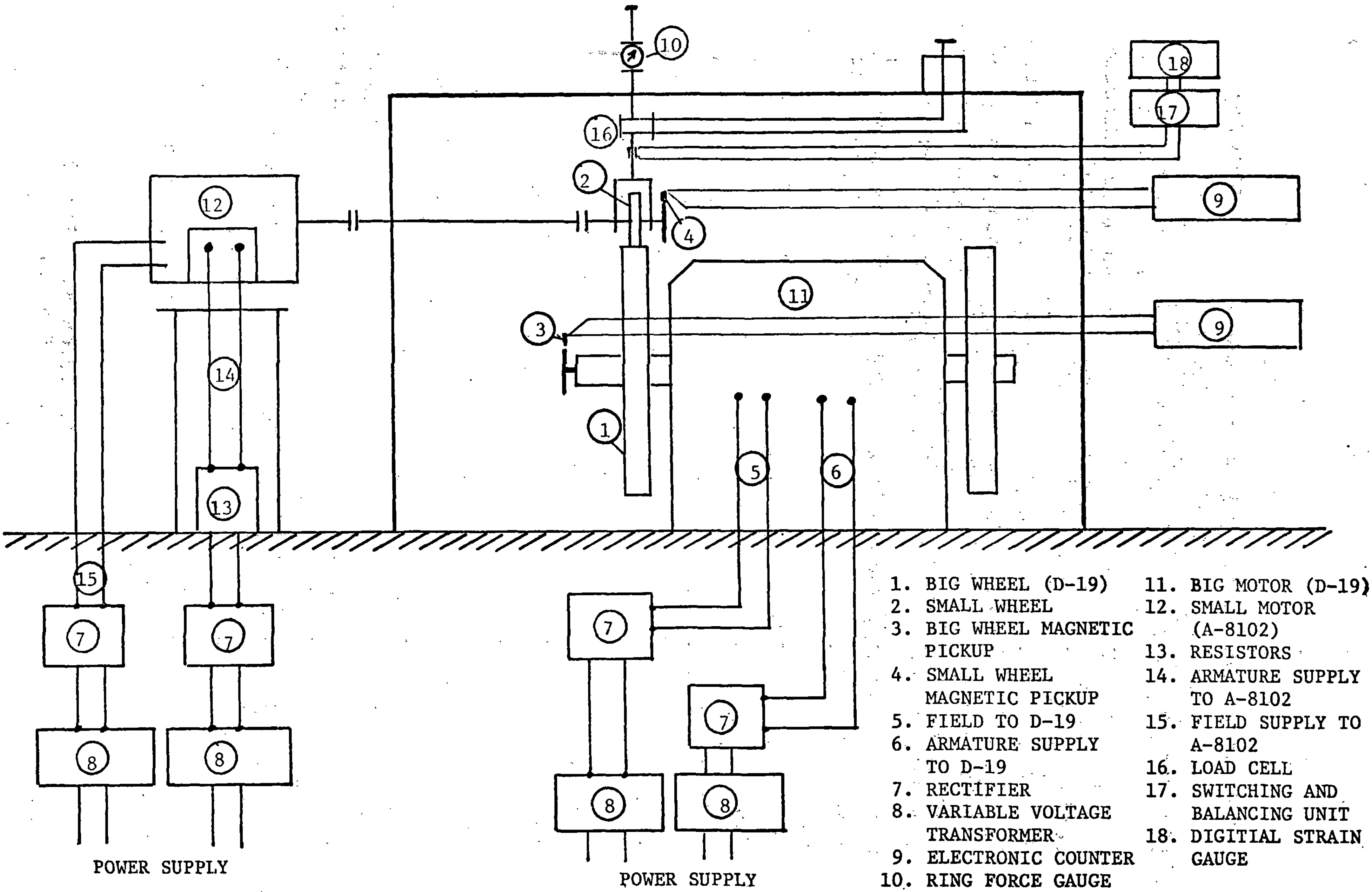

Figure 1. Schematic Arrangement of the DOT-GM EMD-IIT Wheel-Rail Test Facility

vibrations, joints in rail and the like conditions have not been simulated it cannot be said that a steel wheel on a steel rail under similar surface conditions would behave exactly as the tests predict. However, compared to the various other facilities on which experimental work of a similar nature were carried out, this facility can claim to give results which are considered as good a simulation as has been possible so far.

Measurement of Creep

The speed of rotation of each wheel is measured very accurately by means of magnetic pickups Fig. 1 [3 and 4]. A gear having 144 teeth is mounted on the axle of each wheel. Hence, the magnetic pickup senses 144 cycles/revolution. The number displayed by the electronic counters Fig. 1 [9] which are connected to the magnetic pickups is in cycles/sec. The R.P.M. of each wheel can then be calculated as follows:

$$\frac{\text{cycles}}{\text{sec}} \cdot \frac{1}{144} \frac{\text{Revolutions}}{\text{Cycle}} \cdot 60 \frac{\text{Sec}}{\text{Min}} = \frac{\text{Rev}}{\text{Min}}$$

The gap between the gear and the magnetic pickup is kept between .01 and .02 inches.

Knowing the speeds of the two wheels independently at any instant, the creep generated at that instant can be calculated. Creep is generated by braking the small wheel motor Fig. 1 [12] dynamically. This is done by supplying field current Fig. 1 [15] to the small wheel motor. The motor then acts as a generator and the current generated is dissipated as heat through a bank of resistors Fig. 1 [13] connected in parallel to armature.

Measurement of Coefficient-of-Friction

Both the wheels are driven by D.C. motors Fig. 1 [11 and 12]. The electrical circuit consists of a variable transformer Fig. 1 [8] and a rectifier Fig. 1 [7] for the field and armature of each motor. The rectified power is obtained from 230 volts A.C., except for the field of small motors which is supplied by 120 volts A.C. The control and circuit diagram details of the facility are given in a previous technical report.[2] In the central portion of the rig, immediately above the yoke which holds the small wheel is a load cell Fig. 1 [16] consisting of a tube welded to flanges on each end. This load cell consists of three strain gauge bridges for measuring the axial, longitudinal and lateral loads. The gauges are arranged so that each bridge reacts independently.

A BLH Electronics model 1200 portable digital strain indicator Fig. 1 [18] is used to amplify, measure and display the millivolt per volt output of the wire strain gauges in micro inch-per-inch of strain. A BLH Electronics model 1225 switching and balancing unit Fig. 1 [17] is used. This instrument allows all the three strain gauge bridges to be successively monitored on one single above-mentioned strain indicator.

The setup to apply axial load is as shown in the previous report.[2] A force ring gauge Fig. 1 [10] is placed between the central support shaft (which transmits the applied load to the small wheel) and a bolt (which is used to apply the load). By tightening this bolt, force is transmitted via the ring gauge, the support shaft and the load cell on to the small wheel. Ring gauge is used to measure this force because the axial strain gauge bridge did not work up to satisfaction during initial calibration.[2]

Knowing the axial load-N and the longitudinal load-T, the coefficient of friction, $\mu = \frac{T}{N}$ between the big wheel and the small wheel can be calculated.

No attempt has been made to describe every single detail of the test facility in this report. For this, readers are referred to the Bibliography.[1, 2]

III
EXPERIMENTAL INVESTIGATION OF SIMILITUDE LAW

Preparation for Testing

Several preparations had to be made before each experiment could be carried out systematically to yield meaningful and repeatable results.

Preparation of Surface. The surface of the big wheel was finished to around 20 μ_{in}. After every test, a track was formed on the big wheel and so a new surface was used for each experiment by moving the big wheel in the lateral direction. When the entire surface of the big wheel was covered with tracks, a light cut was taken across the wheel. A high speed steel tool was placed in the toolholder which was welded to the base of the rig in front of the wheel and traversed across the wheel while the axle was slowly turned. The wheel was then ground with a tool past grinder and finally polished with 320 and 400 grit emery papers to obtain the desired finish. It was then checked by a surfindicator.

The shape of contact between the two wheels was checked after each experiment and a new small wheel was used when the shape was no longer an ellipse.

Before the start of each experiment, the big and the small wheel were cleaned with trichloroethylene in order to eliminate minute surface impurities and to establish a rolling contact between virgin steel and virgin steel.

Measurement of Big Wheel Diameter. In order to calculate creep, the diameter of both the wheels must be correct to the third decimal place.[2] To obtain this accuracy, the big wheel diameter was measured by means of a "Pi Tape." It is a thin metallic tape consisting of a main scale and a vernier scale. By wrapping it around the circumference of the big wheel, it gives its average diameter up to three places of decimal.

The diameter of the small wheel was measured up to four places of decimal at G.M. E.M.D.

Warming up of the Rig. Before the first experiment of the day could be performed, the big wheel motor was made to run for 40 to 50 minutes to loosen the grease in the gear case and to eliminate initial vibrations of the motor. Tests were begun only after the running of the big motor was perfectly smooth.

Preparation for Zero-Reading (Zero Creep at Zero Tangential Force). The accuracy of the experiment depends on the establishment of zero initial condition. Before the start of each experiment, the lateral and the longitudinal strain gauges were adjusted to zero with the small wheel lifted just a little. Contact was then made between the two wheels, the desired load was applied and the big wheel motor was started. The big wheel was then driving the small wheel and a certain longitudinal force was recorded in the strain indicator. This reading was brought to zero by supplying some power to the small wheel motor. As the strain gauge readings were constantly fluctuating, and an average reading was always taken, it was difficult to get exact zero creep at zero coefficient of friction.

Test Procedure

G. Itami[1] and K. Karamchandani[2] had performed several experiments to find the relationship between creep and coefficient of friction. Similar experiments were performed at various other loads to confirm the relationship and to proceed with nondimensional analysis. The following was the procedure adopted to obtain the above-mentioned data:

1. Preliminary preparations of the test as discussed above were made.

2. Creep was gradually introduced by braking the small wheel. This was done by supplying field current to the small wheel motor.

3. Tangential force developed between the wheels was measured from the strain gauge indicator for every creep.

4. Creep was increased progressively and tangential force measured until the point when gross slipping just began to occur.

5. Braking force was immediately released and the two wheels brought to stop.

Creep developed during the experiment was calculated from the speed of the two individual wheels at various breaking loads.

$$\text{Creep } (\xi) = 1 - \frac{\omega_s}{\omega_B} \cdot \frac{R_s}{R_B}$$

$$= 1 - \frac{N_s}{N_B} \cdot \frac{R_s}{R_B}$$

Where:

N_S = Speed on small wheel in R.P.M.

N_B = Speed on big wheel in R.P.M.

R_S = Radius of small wheel in inches

R_B = Radius of big wheel in inches

In a prolonged laboratory test, the large and the small wheel show wear. The radii R_S and R_B are thus reduced by a small amount. The percentage change in R_S is, however, more. It can be shown that the observed maximum change in R_S by 0.0003 will affect the creep (ξ) by 0.0000588. (See Appendix A.) The creep values thus obtained are considered accurate up to fourth decimal place and maximum error in fifth decimal is 6.

Coefficient of friction at each value of creep was obtained by dividing tangential force (T) by normal force (N).

$$\text{Coefficient of friction } (\mu) = \frac{T}{N}\,.$$

During the entire test, the speed of the big wheel was kept near 50 R.P.M. As the experiment progressed, the speed of the big wheel dropped and had to be increased. This was done by increasing the armature supply to the big wheel motor.

Graphically obtained average creep curves are shown in Figures 2, 3, 4, 5 and 6. The experimental data from which the above curves were obtained are shown in Appendix B.

The creep curves can be represented in a dimensionless form by plotting the values of $\frac{T_x}{\mu' N}$ versus $\frac{Gab\xi_x}{\mu' N}$, where:

G	=	Shear modulus
a, b	=	Semi axis of contact ellipse
ξ_x	=	Longitudinal creep
T_x	=	Tangential force in longitudinal direction
μ'	=	Coefficient of friction relating the maximum tangential force that can be transmitted without gross slipping
N	=	Normal force

For perfectly smooth surfaces, the values of semi axis of the contact ellipse can be obtained from the Hertz theory.[4] However, in our case, as the experiment progresses the surface of the big and the small wheel get worn and the actual area of contact is larger than the theoretical one calculated from the Hertz theory (Fig. 9).

In order to represent our experimentally-obtained creep curves in dimensionless fashion, the semi axis of contact was calculated as follows: The width of the track formed on the small wheel was measured after each experiment. This was taken as the minor axis '2b' of the contact ellipse. As the profile on the small wheel was so made that the ratio of major to minor axis of contact ellipse equals 1.57 (see Appendix A), the major axis, '2a' could be obtained. That the ratio of a/b is actually around 1.57 could be checked from Table 5 which represents an independent experiment done for another purpose.

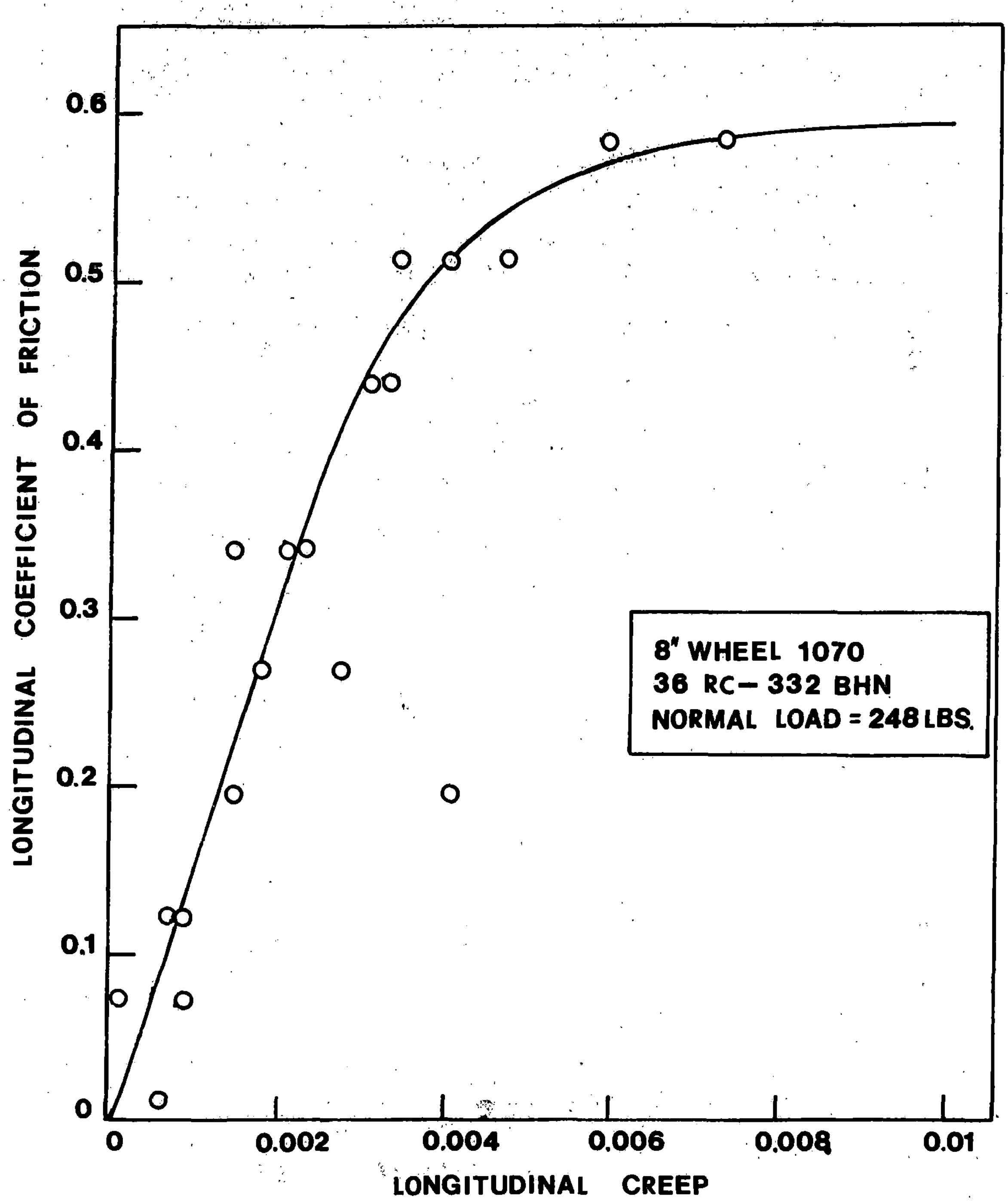

Figure 2. Longitudinal Coefficient of Friction vs. Longitudinal Creep

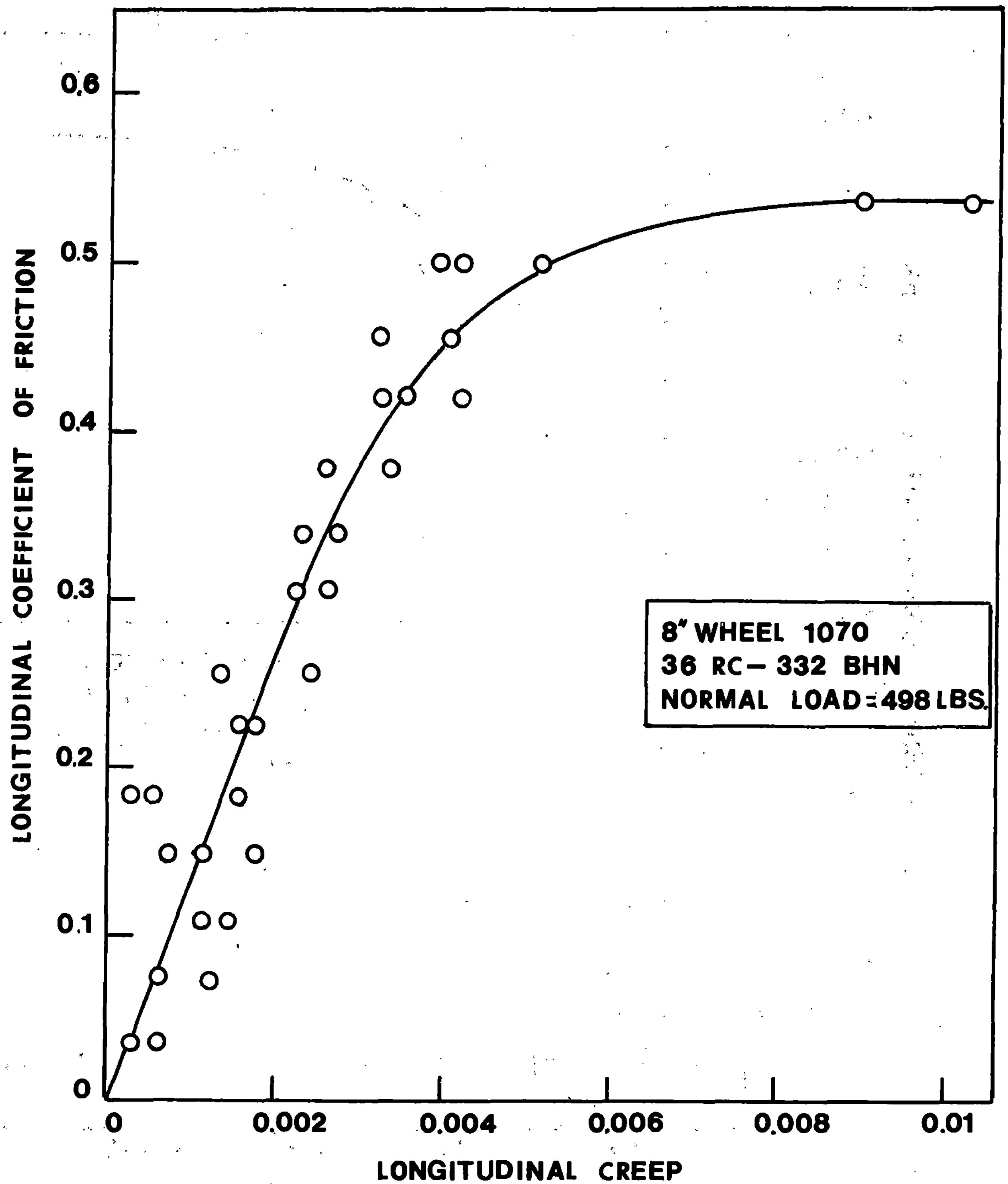

Figure 3. Longitudinal Coefficient of Friction vs. Longitudinal Creep

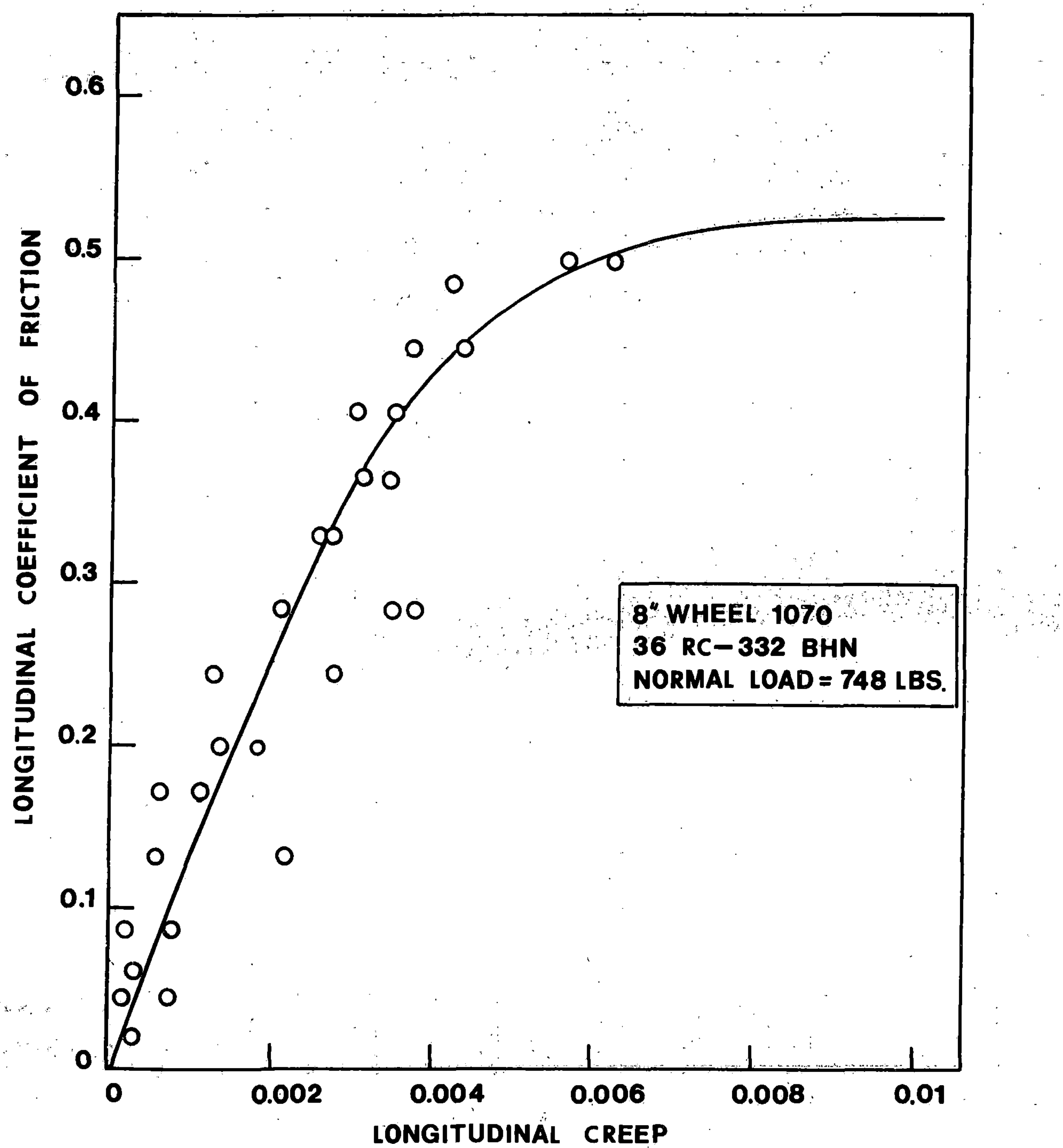

Figure 4. Longitudinal Coefficient of Friction vs. Longitudinal Creep

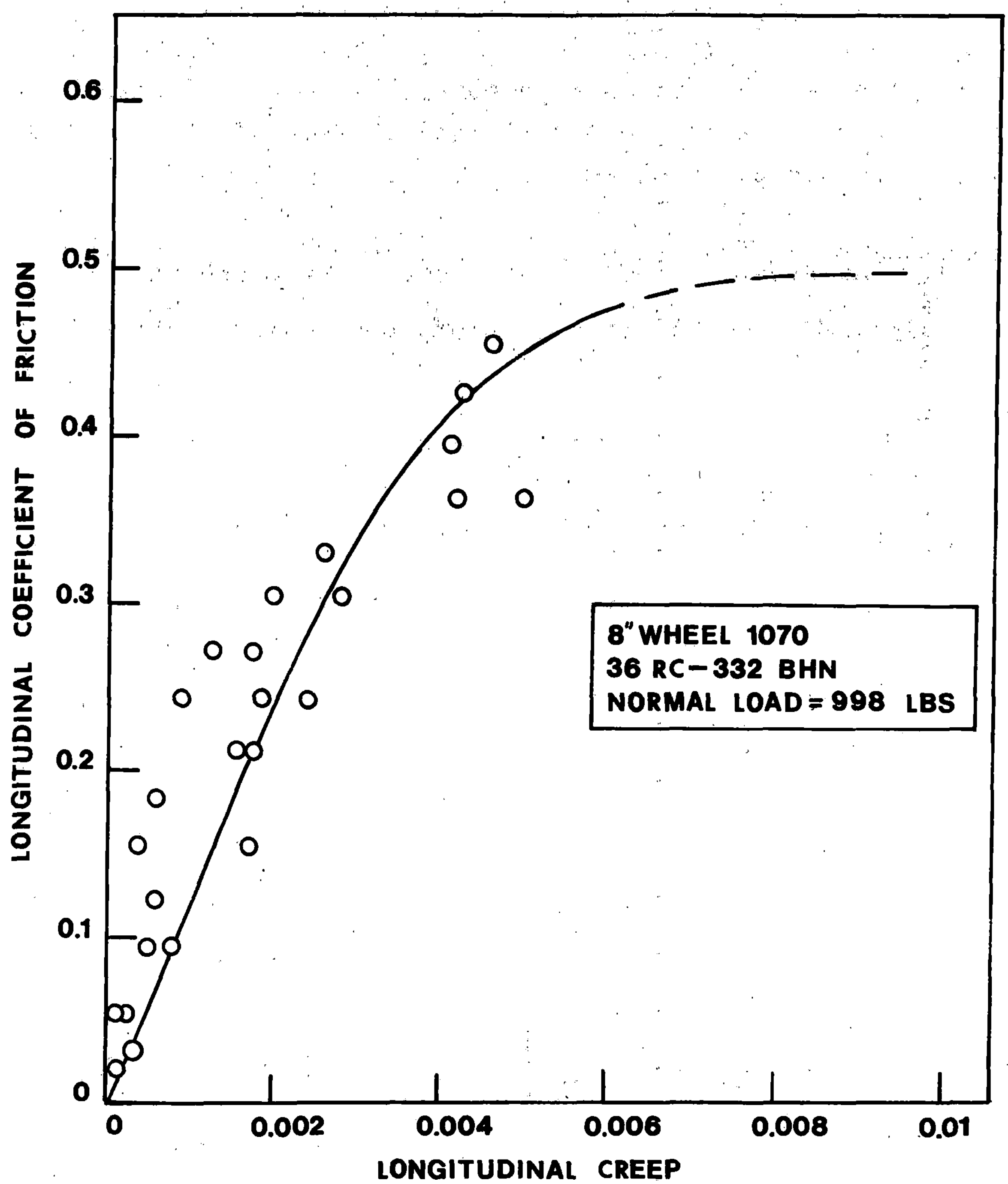

Figure 5. Longitudinal Coefficient of Friction vs. Longitudinal Creep

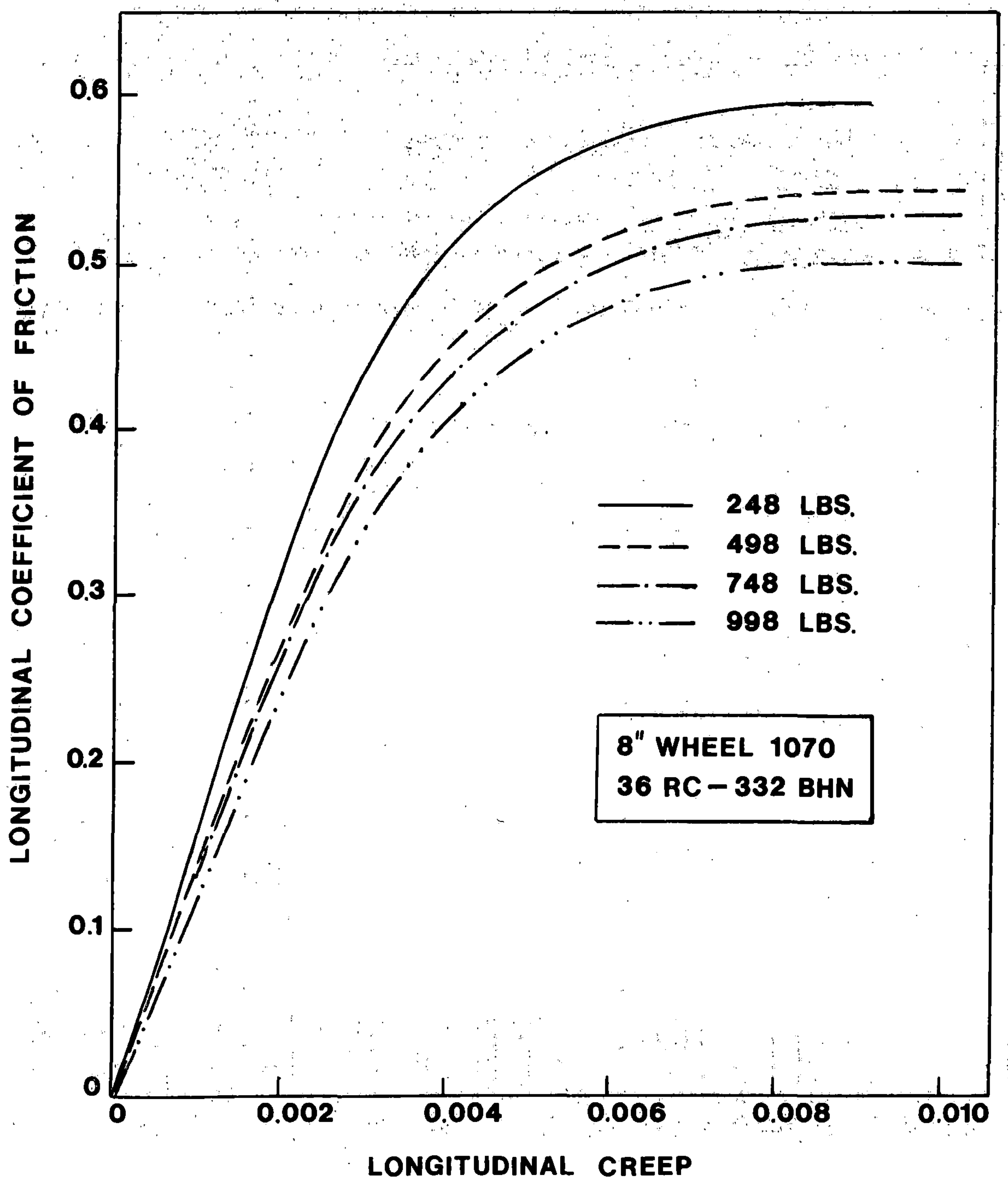

Figure 6. Longitudinal Coefficient of Friction vs. Longitudinal Creep

The calculations of the two dimensionless parameters for various loads have been tabulated in Tables 1 through 4.

Test Results

Creep curves obtained during the experiments are compared with those obtained previously by G. Itami[1] and K. Karamchandani[2] (Fig. 7). The slope of the curves in the microslip region is the same in all the three casees. However, the plateaus of the present curves are slightly lower. Following may be some reasons for obtaining lower plateaus:-

1. It has been observed by Verbeeck[5] that on absolutely clean rails, the maximum coefficient of friction decreases from .7 to .6 if the relative humidity varies between 30 and 70%.

2. For the present study, the big wheel was machine cut, ground and then polished whereas for previous studies, the wheel was machine cut and polished. This difference in the method of preparing the surface may have caused a difference in the final testing surface which in turn may have given lower plateaus.

The maximum coefficient of friction that can be attained decreases with the increase in load (Fig. 8). However, the rate of decrease goes down with the increase in load. It can, therefore be observed that the method of increasing the tractive effort by increasing the load is more efficient at higher operating loads than at lower operating loads. Under the present simulated conditions 889 lb corresponds to the operating loads of G.M. E.M.D. vehicles.

Fig. 9 shows the variation of theoretical and actual area of contact. The theoretical area is calculated from the Hertz theory[4] (see Appendix A). It is the area obtained when two perfectly smooth bodies come in contact. The actual (or experimental or true) contact is that which is present after the two wheels have rolled in contact and are therefore worn. Fig. 10 shows that the actual area of contact is 1.8 to 2.2 times the theoretical area.

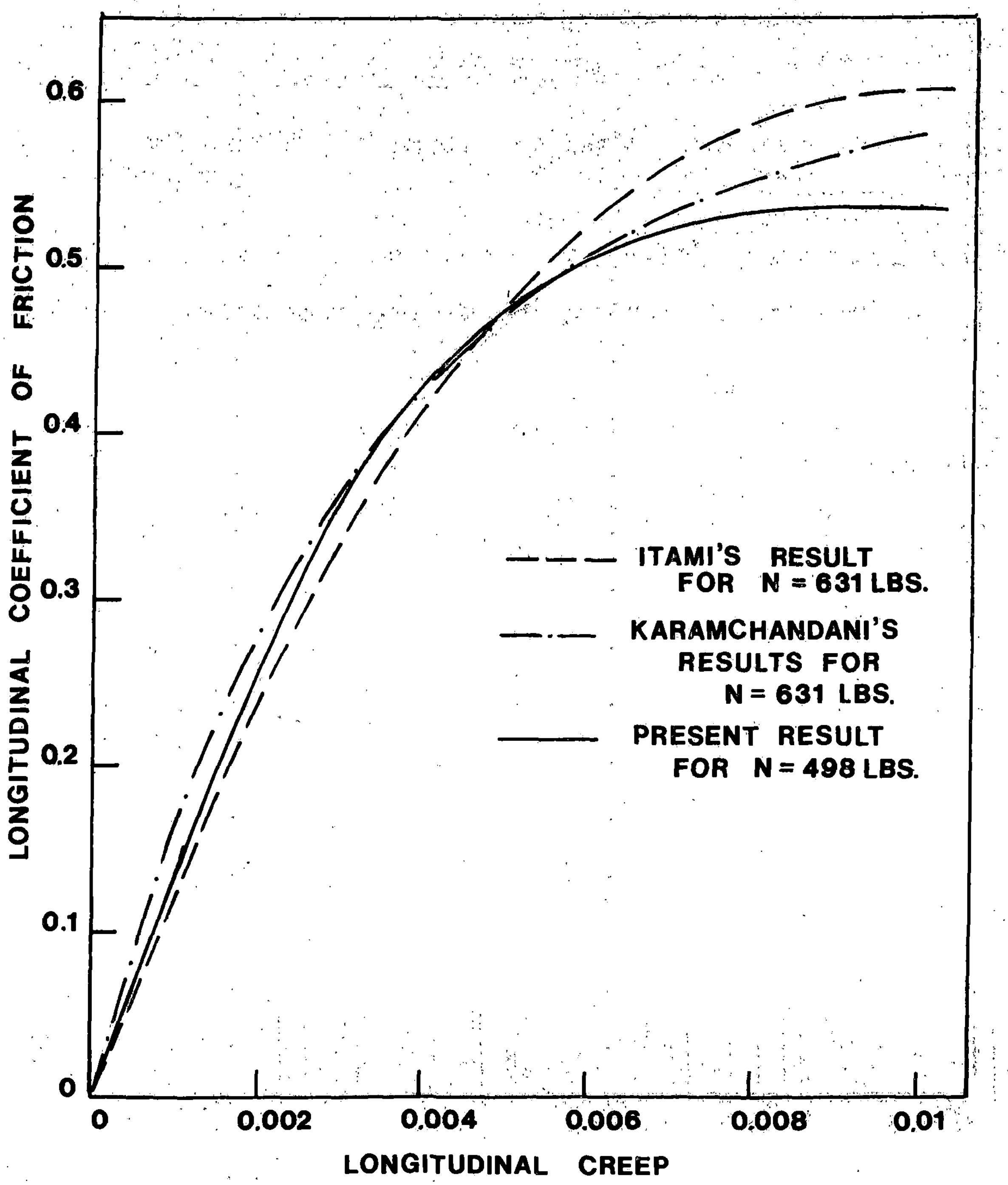

Figure 7. Longitudinal Coefficient of Friction vs. Longitudinal Creep

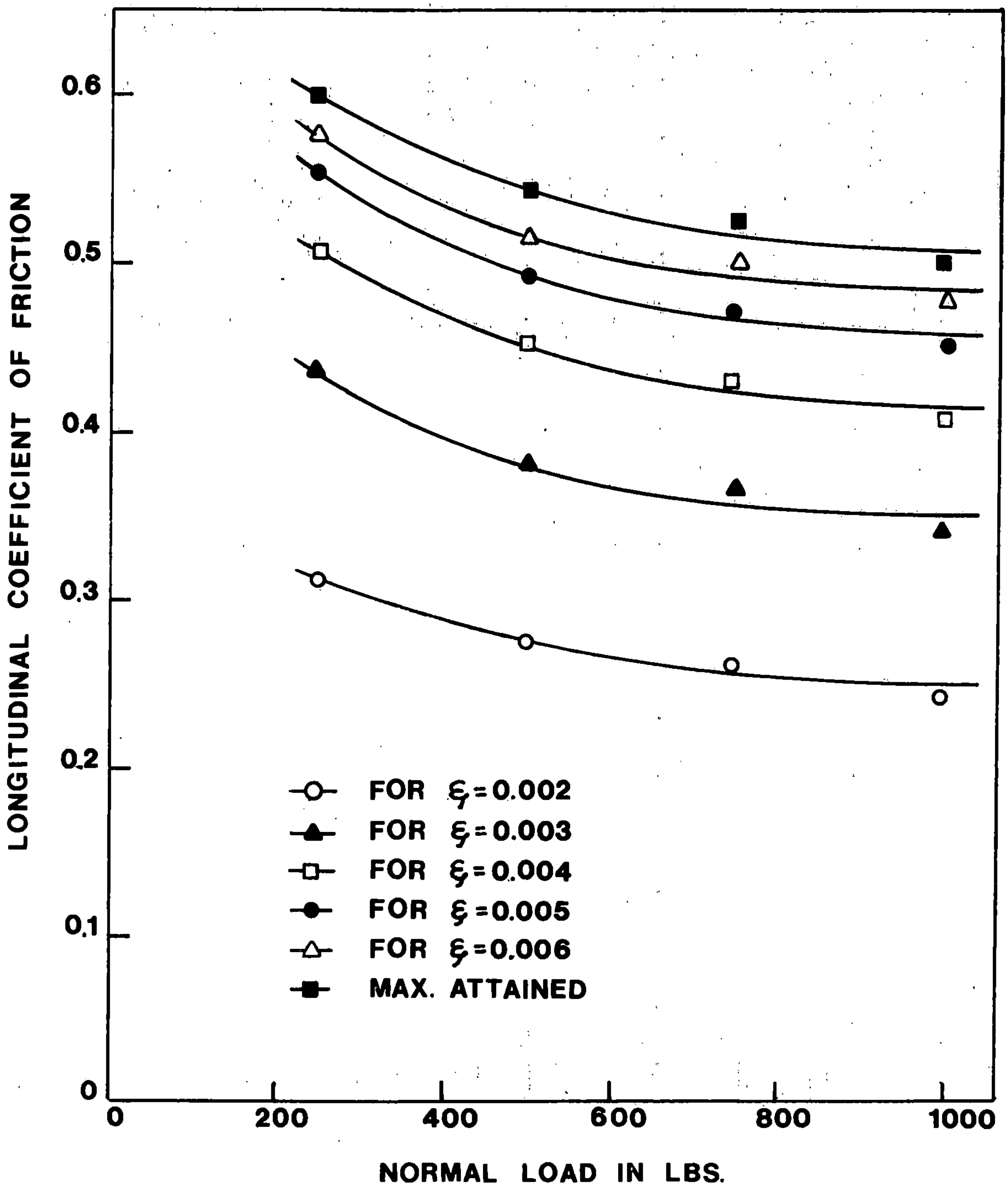

Figure 8. Longitudinal Coefficient of Friction vs. Normal Load

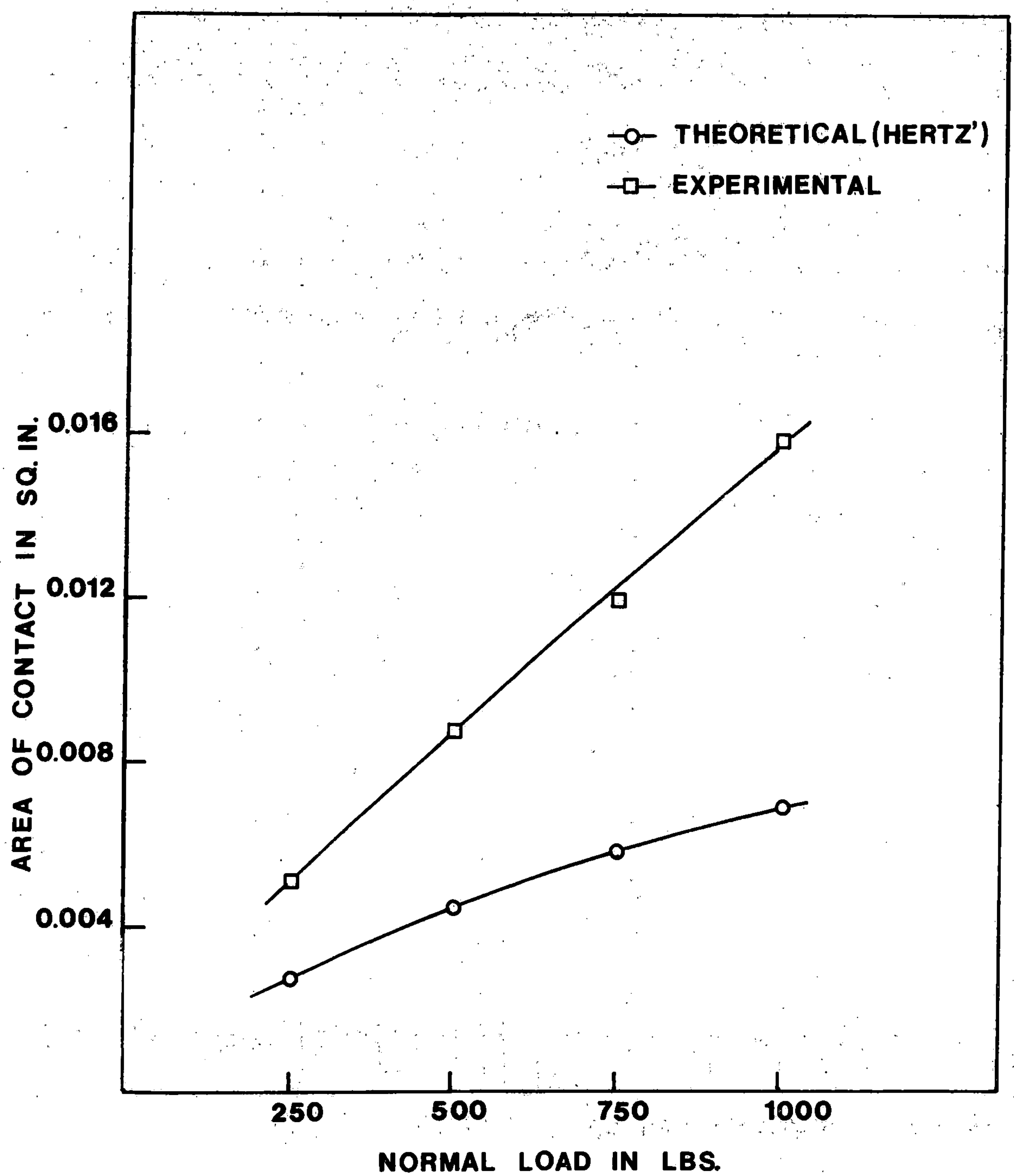

Figure 9. Area of Contact vs. Normal Load

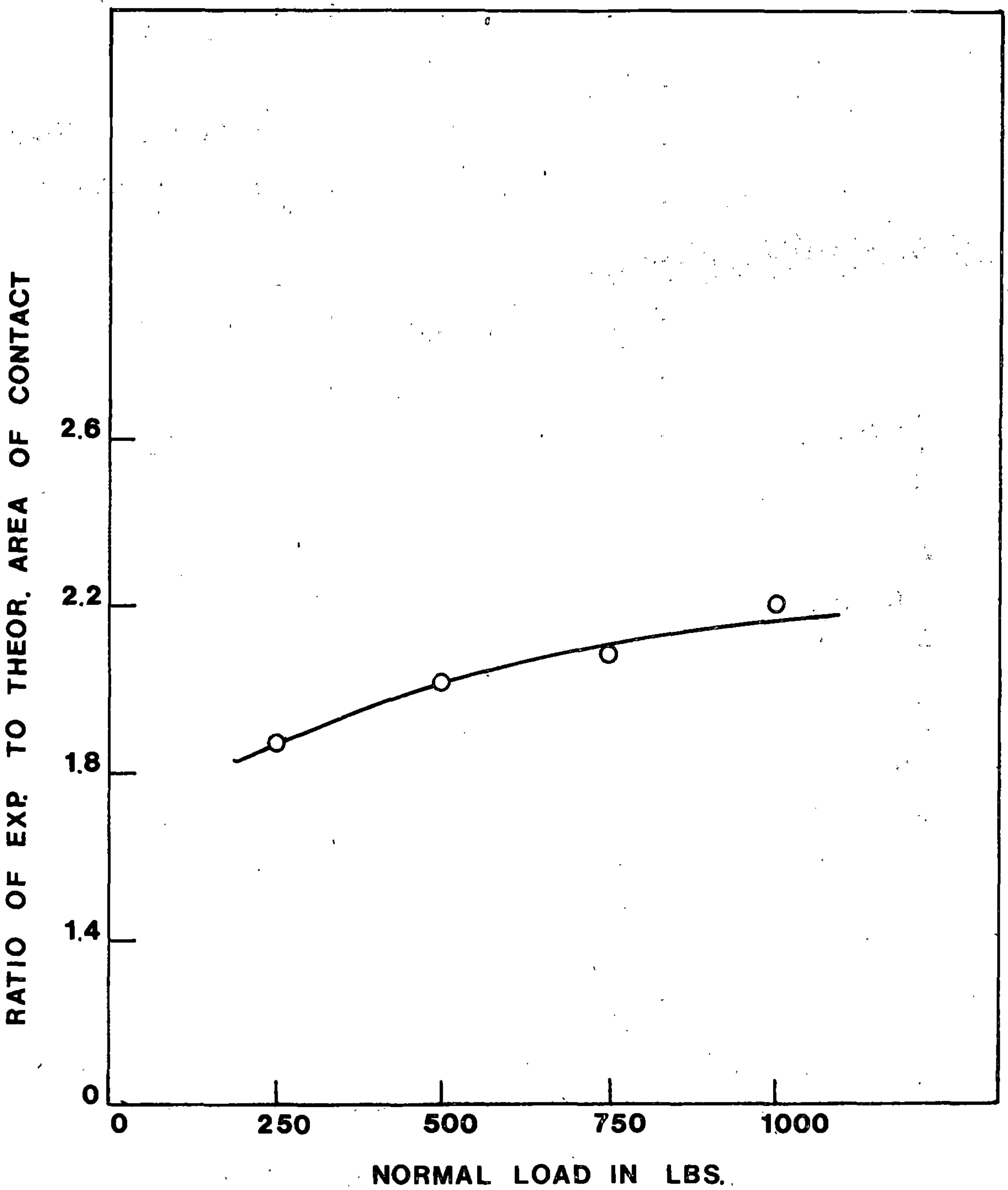

Figure 10. Ratio of Experimental to Theoretical Area of Contact vs. Normal Load

The plots for $\frac{T_x}{\mu' N}$ versus $\frac{Gab\xi_x}{\mu' N}$ for all the loads fall on one single curve as shown in Fig. 11. This curve also coincides with the theoretical curve of Kalker.[6] It can therefore be concluded that the law of similitude holds good not only for perfectly smooth surfaces, but also for surfaces that get worn with advancement of time. The area of contact, however, should be the actual area of contact after the wear has taken place. The theoretical area of contact if used, will not make all the curves to fall on one single nondimensional curve. It, therefore, seems that as the wear progresses with time and the area of contact increases, the creep generated at a particular load and coefficient of friction decreases to a value less than what it would be if the wear did not take place. It was therefore suspected at this stage that the product of area times creep for a given load and a given coefficient of friction is approximately constant with time.

Because of the above observation it was desired to have a thorough understanding of the variation of area of contact and creep with time as well as the rate and the nature of wear taking place with time. A plan for a complete parametric study was therefore laid out and is discussed in detail in Chapter IV.

Table 1. Nondimensional Values for Test With Normal Load = 248 lb.

Semi major axis (a) = .050448 in.
Semi minor axis (b) = .0321325 in.

$$\frac{T}{\mu' N} = \frac{\mu}{\mu'} = \frac{\mu}{.599}$$

$$\frac{G \times a \times b \times \xi}{\mu' N} = \frac{11 \times 10^6 \times .0321325 \times 050448 \times \xi}{.599 \times 248}$$

$$= 120.0172 \times \xi$$

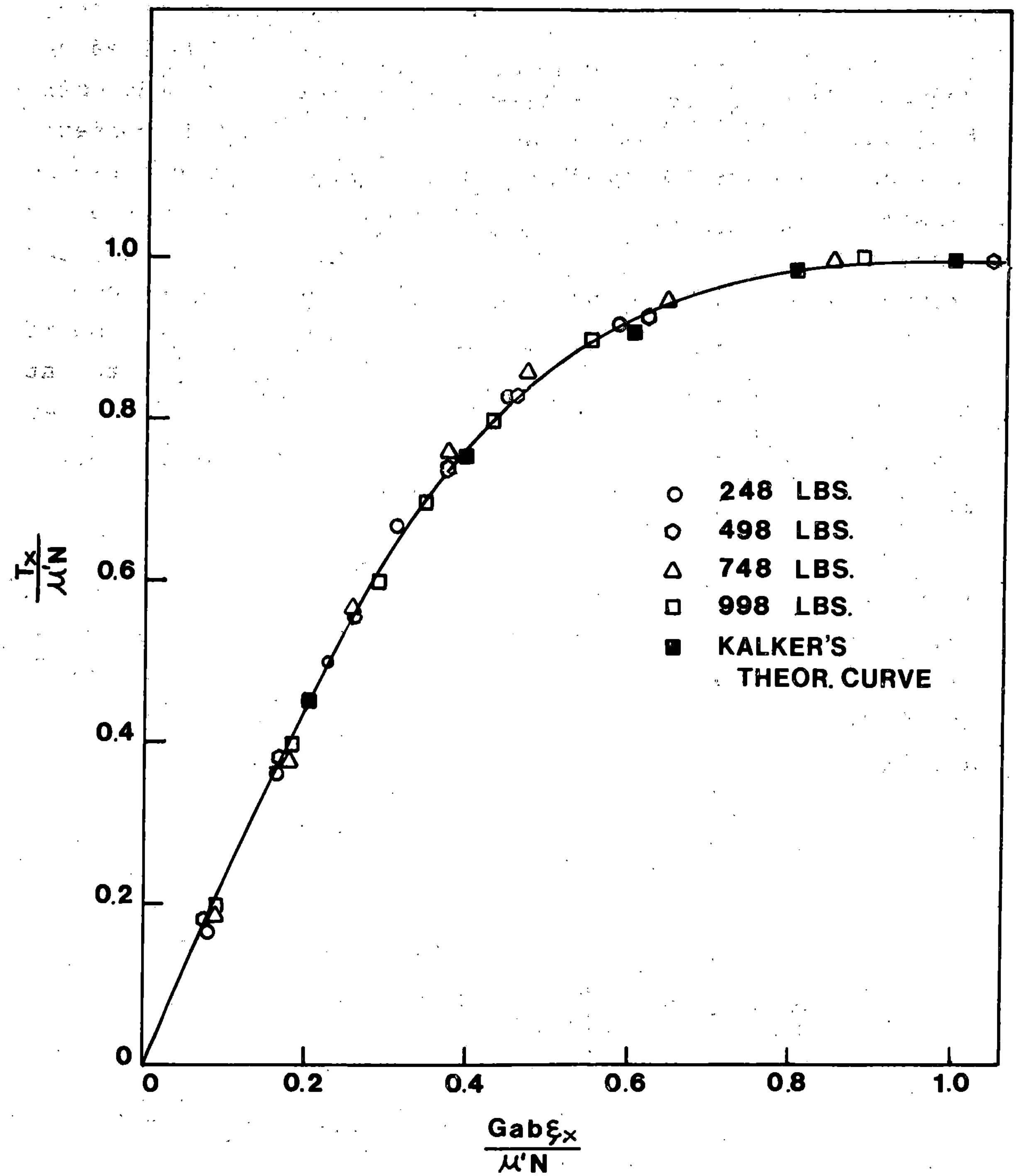

Figure 11. Nondimensional Creep Curve

No.	μ	ξ	$\frac{T}{\mu' N} = \frac{\mu}{.599}$	$\frac{Gab\xi}{\mu' N} = 120.0172 \times \xi$
1	.10	.00065	.1669449	.0780111
2	.20	.0013	.3338898	.1560223
3	.30	.0019	.5008347	.2280326
4	.40	.00263	.6677796	.3156452
5	.45	.00307	.751252	.3684528
6	.50	.0037	.8347245	.4440636
7	.55	.00485	.9181969	.5820834
8	.599	.009	1.000	1.0801548

Table 2. Nondimensional Values for Test With Normal Load = 498 lb.

Semi major axis (a) = .0668421 in.
Semi minor axis (b) = .0425746 in.

$$\frac{T}{\mu' N} = \frac{\mu}{\mu'} = \frac{\mu}{.5375}$$

$$\frac{G \times a \times b \times \xi}{\mu' \times N} = \frac{11 \times 10^{6} \times .0668421 \times 0425746}{.5375 \times 498}$$

No.	μ	ξ	$\frac{T}{\mu' N} = \frac{\mu}{.5375}$	$\frac{Gab\xi}{\mu' N} = 116.93985 \times \xi$
1	.10	.00075	.1860465	.087706
2	.20	.00146	.372093	.1707321
3	.30	.00225	.5581395	.2631146
4	.40	.0032	.744186	.3742075
5	.45	.0039	.8372093	.4560654
6	.50	.00525	.9302325	.6139342
7	.5375	.009	1.00	1.0524586

Table 3. Nondimensional Values for Test With Normal Load = 748 lb.

Semi major axis (a) = 0771841 in.
Semi minor axis (b) = 0491619 in.

$$\frac{T}{\mu' N} = \frac{\mu}{\mu'} = \frac{\mu}{.525}$$

$$\frac{G \times a \times b \times \xi}{\mu' \times N} = \frac{11 \times 10^{6} \times .0771841 \times .0491619 \times \xi}{.525 \times 748}$$

$$= 106.28504 \times \xi$$

No.	μ	ξ	$\frac{T}{\mu' N} = \frac{\mu}{.525}$	$\frac{Gab\xi}{\mu' N} = 106.28504 \times \xi$
1	.10	.0008	.1904761	.085028
2	.20	.0016	.3809523	.170056
3	.30	.0024	.5714885	.255084
4	.40	.0035	.7619047	.3719976
5	.45	.0044	.8571428	.4676541
6	.50	.0060	.9523809	.6377102
7	.525	.008	1.00	.86028

Table 4. Nondimensional Values for Test With Normal Load = 998 lb.

Semi major axis (a) = .0889248 in.
Semi minor axis (b) = .05664 in.

$$\frac{T}{\mu' N} = \frac{\mu}{\mu'} = \frac{\mu}{.50}$$

$$\frac{G \times a \times b \times \xi}{\mu' \times N} = \frac{11 \times 10^6 \times .0889248 \times .05664 \times \xi}{.50 \times 998}$$

$$= 111.02637 \times \xi$$

No.	μ	ξ	$\frac{T}{\mu' N} = \frac{\mu}{.50}$	$\frac{Gab\xi}{\mu' N} = 111.02637 \times \xi$
1	.10	.00082	.2	.0910416
2	.20	.00165	.4	.1831935
3	.30	.0026	.6	.2886685
4	.35	.00313	.7	.3475125
5	.40	.00383	.8	.4252309
6	.45	.00493	.9	.54736
7	.497	.008	1.0	.8882109

IV

PARAMETRIC STUDY OF FRICTION-CREEP

A detailed systematic study of the variations of different parameters with time was found absolutely necessary to understand friction creep phenomenon and to explain the results obtained in the previous chapter on a theoretical basis.

Preparation for Testing

All the preparations made before conducting the previous set of experiments were made before the start of each of these experiments. Some additional preparations were also made.

Method of Obtaining True Width. It was desired to obtain the width of the track on the small wheel with reasonably high accuracy. This was accomplished by obtaining a replica of a portion of the track on the small wheel. This replica was then observed under the microscope and the width of the tract (b_T) was measured up to four decimal places. The replica was made by pouring a mixture of acrylic powder and acrylic liquid into a specially-prepared mould that fits on the wheel. The so-formed paste solidifies within five minutes, giving a perfect replica of the surface.

Method of Obtaining True Area of Contact. As the present test required the two wheels to roll for an extended period of time, it was observed that the area of contact no longer remains an ellipse. The area tends to approach a rectangle. Hence, at any time during the experiment, the true shape of the area of contact was anywhere between an ellipse and a rectangle (Fig. 12). A similar observation was made by Dr. H. I. Andrews.[7] It was necessary to measure this true area of contact. This proved quite difficult and a number of alternative methods had to be rejected before the following method could be accepted.

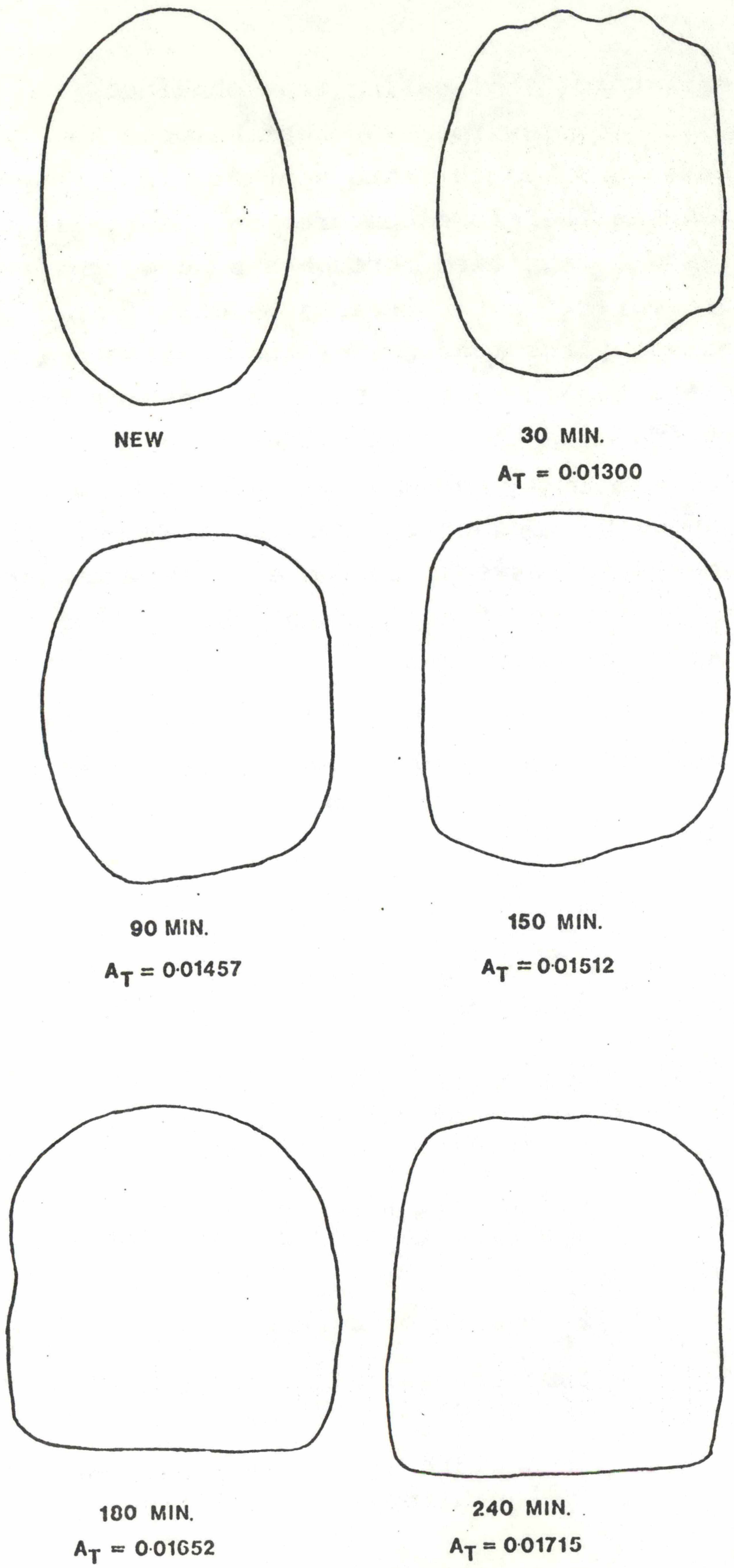

Figure 12. Variation of Area of Contact with Time.
(N = 548 lb, μ = 0.46)

A piece of replicating tape obtained from Ernest F. Fullam, Inc. of New York was kept between the two wheels and the wheels were brought into contact. The shape of the contact area was therefore captured on the replicating tape. This area was magnified through a shadowgraph and was measured by a planimeter. Let this area be called A_R. The A_R value is affected by the presence of the smooth replicating tape between the two surfaces. The thickness of the tape (5 mils), tends to increase the above value whereas the presence of the 'smooth' tape tends to suppress the increase in the above value caused by roughness generated by wear. There will be some compromise between the two effects somewhere, but the value A_R is not the true value of the area of contact, and hence has to be corrected.

The area of contact, as mentioned earlier, is between an ellipse and a rectangle. Hence, we can write:

$$A_R = X_1 \times \frac{a_R}{2} \times \frac{b_R}{2} \qquad (1)$$

and

$$A_T = X_2 \times \frac{a_T}{2} \times \frac{b_T}{2} \qquad (2)$$

where

a_R = length of contact area in the direction of rolling obtained from the replica,

b_R = width of contact area perpendicular to the direction of rolling obtained from the replica,

A_T = true area of contact,

a_T = true length of contact area in the direction of rolling,

b_T = true width of contact area perpendicular to the direction of rolling.

X_1 and X_2 are constants whose values are varied from 3.14 to 4. Dividing Equation (2) by (1), we get:

$$A_T/A_R = (X_1/X_2)\ (a_T/a_R)\ (b_T/b_R) \tag{3}$$

Experimental measurements of b_R and A_R for different N (Table 5) of elliptical contact for smooth surfaces as measured on the replica tape show that a_R/b_R is nearly constant (1·5-1·6). The shape of the ellipse of contact thus remained unchanged. It can therefore be assumed that the shape obtained on the replica is similar to the shape of the true area of contact with only the size varying. Thus,

$$X_1 = X_2 \text{ and } a_T/a_R = b_T/b_R$$

Hence, Equation (3) can be written as:

$$A_T = A_R\ (b_T\ b_R)^2 \tag{4}$$

b_R is measured from the replica by the shadograph and b_T is measured as discussed in the previous section of this chapter.

To verify this method of obtaining true area, an experiment was performed whereby area of contact was measured by the above method between new wheels at various loads. The graph of obtained area was plotted and compared with theoretical area for perfectly smooth surfaces (Fig. 13). The two curves were quite close, especially at higher loads showing that the above method was an acceptable one.

Calculations of true area for loads of 548 lb., 748 lb., and 1000 lb. are shown in Tables 6 through 8.

Test Procedure

All tests were performed at three different loads - 548 lb., 748 lb., and 1000 lb. At each load, the test was performed for four different coefficient of friction - 0.15, 0.30, 0.40 and 0.46. For each coefficient of friction, the test was performed for a period of 270 minutes. Creep and area of contact were measured and replicas were taken, at intervals of about 45 minutes.

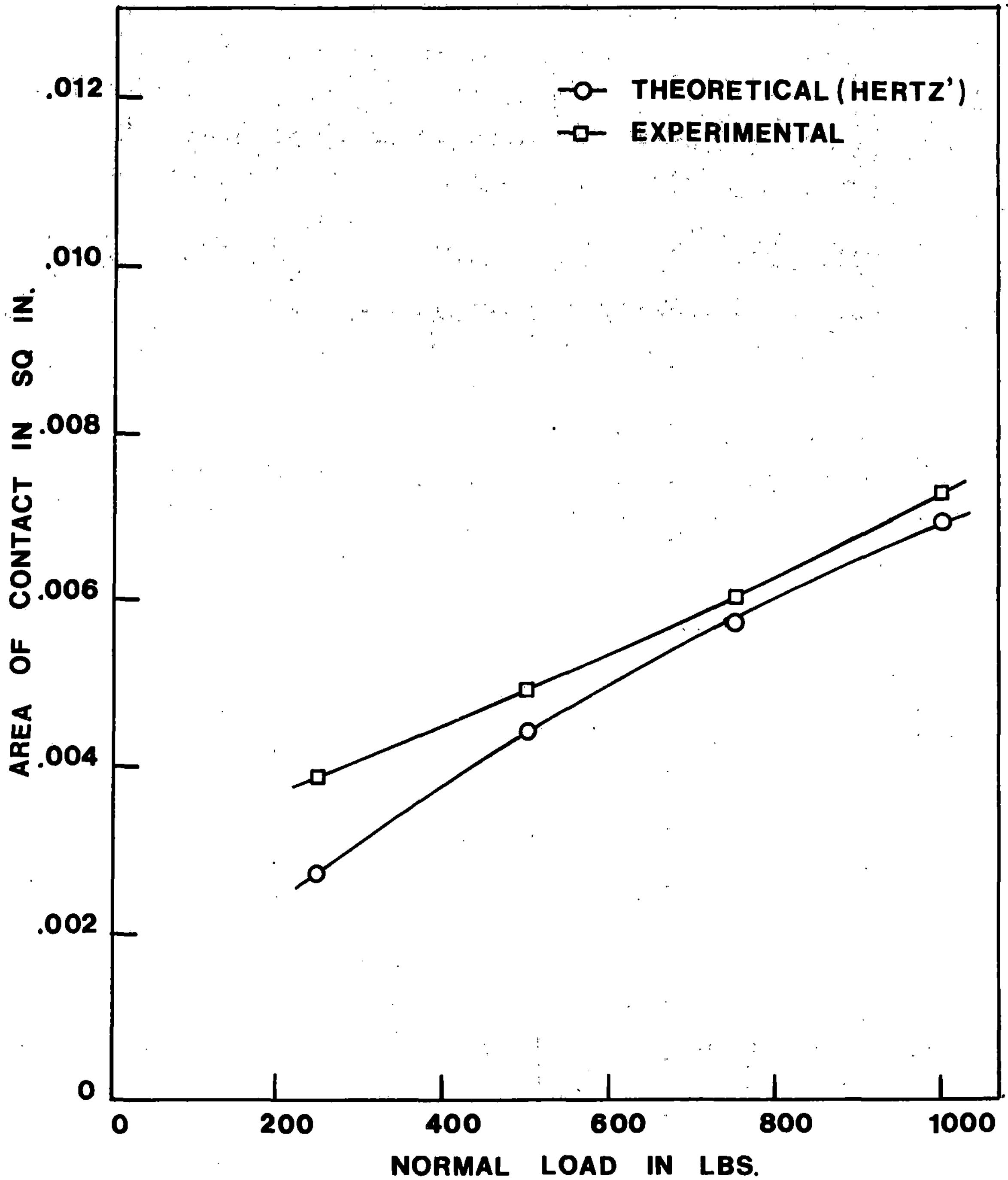

FIGURE 13. AREA OF CONTACT VS. NORMAL LOAD FOR SMOOTH NEW SURFACES.

Following is the operating procedure adopted in conducting the above-mentioned tests:

1.) Preliminary preparations for testing as discussed before were made.

2.) Required load was applied.

3.) Calculated amounts of tangential force was introduced by braking the small wheel dynamically such that the required coefficient of friction was attained.

4.) After every 45 minutes, creep generated was recorded and the machine was stopped.

5.) A replica of the contact area was taken as were also the castings of the worn track of the big and small wheel.

6.) The machine was restarted and run for 45 more minutes after which the entire procedure was repeated.

Precautions. The application of the required tangential load was done very gradually over a period of approximately three minutes to ensure that there was no slippage due to a sudden application of tangential load.

The applied tangential load was observed to be falling slightly with time. Hence, it was checked and increased whenever necessary to keep the generated coefficient of friction at a desired constant level.

The readings on the counter were constantly fluctuating. Hence a mean of the creep obtained during the last three minutes was taken.

As the small wheel motor was acting as a generator and was constantly supplying current to the bank of resistors, the resistors were getting overheated. Therefore a cooling fan was installed to constantly cool the resistors. Also, high-powered cables were used to connect the resistors across the armature.

The speed of the big motor was constant within one R.P.M. for the entire set.

Test Results

All of the test data obtained is tabulated in Appendix B and is also plotted in the form of graphs in Figures 14 through 26. It was interesting to observe that for a constant load and a constant coefficient of friction, the product of creep and coefficient of friction remained fairly constant. For the same load, the constant increased with the increase in coefficient of friction and for the same coefficient of friction, the constant increased with the increase in load. Therefore it appears that when two wheels (or for that matter a wheel on a rail) rolls for an extended period of time with a constant load and at a constant coefficient of friction, the area of contact increases due to wear and the value of creep generated decreases such that the product of area of contact times creep is always a constant.

Table 5. Calculation of Experimental Area of Contact for New Surfaces

Load (lb.)	Area From Replica A_R (sq. inches)	True Width of Track b_T (inches)	Width From Replica b_R (inches)	$K=\frac{b_T}{b_R}$	True Area $A_T = A_R K^2$ (sq. inches)
240	.004684	.05687	.06181	.9200	.003965
498	.008955	.06350	.0850	.7470	.004997
748	.011167	.06340	.094	.7382	.006087
998	.01642	.0790	.11811	.6688	.007346

Table 6. Calculation of True Area of Contact for Normal Load = 548 lb.

Time	Area From Replica A_R (sq. inches)	True Width of Track b_T (inches)	Width From Replica b_R (inches)	$K = \frac{b_T}{b_R}$	True Area $A_T = A_R K^2$ (sq. inches)
		For Coefficient of Friction = .15			
60	.0142	.0705	.119	.5924	.004983
120	.01435	.0939	.112	.8383	.01008
180	.014475	.1032	.118	.8745	.01107
240	.01475	.1110	.119	.9327	.01283
300	.020025	.1192	.144	.8277	.01385
		For Coefficient of Friction = .30			
45	.0141	.0894	.109	.8201	.00948
90	.0155	.1056	.123	.8585	.01142
135	.015675	.1174	.126	.9317	.01360
165	.01585	.1201	.130	.9238	.01352
210	.016525	.1268	.129	.9829	.01596
270	.01845	.1299	.138	.9413	.01634
		For Coefficient of Friction = .40			
30	.0148	.1030	.114	.9035	.01210
75	.0151	.1120	.118	.9491	.01360
120	.01525	.1215	.122	.9959	.01524
165	.015375	.1272	.123	1.0341	.01644
210	.017675	.1336	.135	.98962	.01731
		For Coefficient of Friction = .46			
30	.01502	.1070	.115	.3304	.01300
90	.01522	.1135	.116	.9784	.01457
150	.01537	.1220	.123	.9918	.10512
180	.01565	.1305	.127	1.02755	.01652
240	.017125	.1351	.135	1.00740	.01715

Table 7. Calculation of True Area of Contact for Normal Load = 748 lb.

Time	Area From Replica A_R (sq. inches)	True Width of Track b_T (inches)	Width From Replica b_R (inches)	$K = \frac{b_T}{b_R}$	True Area $A_T = A_R K^2$ (sq. inches)
		For Coefficient of Friction = .15			
45	.01537	.0689	.112	.6151	.00581
90	.01587	.0842	.114	.7385	.00866
135	.0160	.0963	.117	.8230	.01083
180	.0162	.1035	.122	.8483	.011659
225	.01665	.1123	.124	.9056	.01365
270	.01815	.1179	.129	.9139	.01516
		For Coefficient of Friction = .30			
45	.01580	.0997	.115	.8669	.01187
90	.01605	.1126	.117	.9623	.01486
135	.0165	.1254	.126	.9952	.01624
180	.01775	.1396	.140	.9971	.01764
225	.01872	.1458	.146	.9986	.01867
270	0.0201	.1507	.150	1.00466	.02031
		For Coefficient of Friction = .40			
60	.016125	.1061	.117	.9068	.01326
120	.01774	.1305	.137	.9525	.01610
180	.018125	.1416	.143	.9902	.01777
240	.01875	.1472	.145	1.0151	.01932
		For Coefficient of Friction = .46			
45	.01667	.1090	.119	.9159	.01399
135	.01775	.1357	.139	.9762	.01691
165	.01855	.1423	.145	.9813	.01786
210	.01865	.1502	.153	.9816	.01797
255	.0192	.1545	.157	.9840	.01859

Table 8. Calculation of True Area of Contact for Normal Load = 1000 lb.

Time	Area From Replica A_R (sq. inches)	True Width of Track b_T (inches)	Width From Replica b_R (inches)	$K = \frac{b_T}{b_R}$	True Area $A_T = A_R K^2$ (sq. inches)
		For Coefficient of Friction = .15			
45	.01732	.0936	.119	.7865	.010718
90	.01760	.1033	.124	.8330	.012214
135	.01810	.1067	.127	.8401	.01267
180	.01877	.1144	.134	.8537	.01368
225	.01927	.1199	.137	.8751	.01476
270	.01962	.1224	.141	.8680	.01478
		For Coefficient of Friction = .30			
45	.01847	.1136	.130	.8738	.01410
90	.01975	.1190	.132	.9015	.01605
135	.02082	.1300	.143	.9090	.01721
180	.02122	.1406	.150	.9373	.01864
225	.02155	1446	.154	.9389	.01899
270	.022625	.1516	.161	.9416	.02006

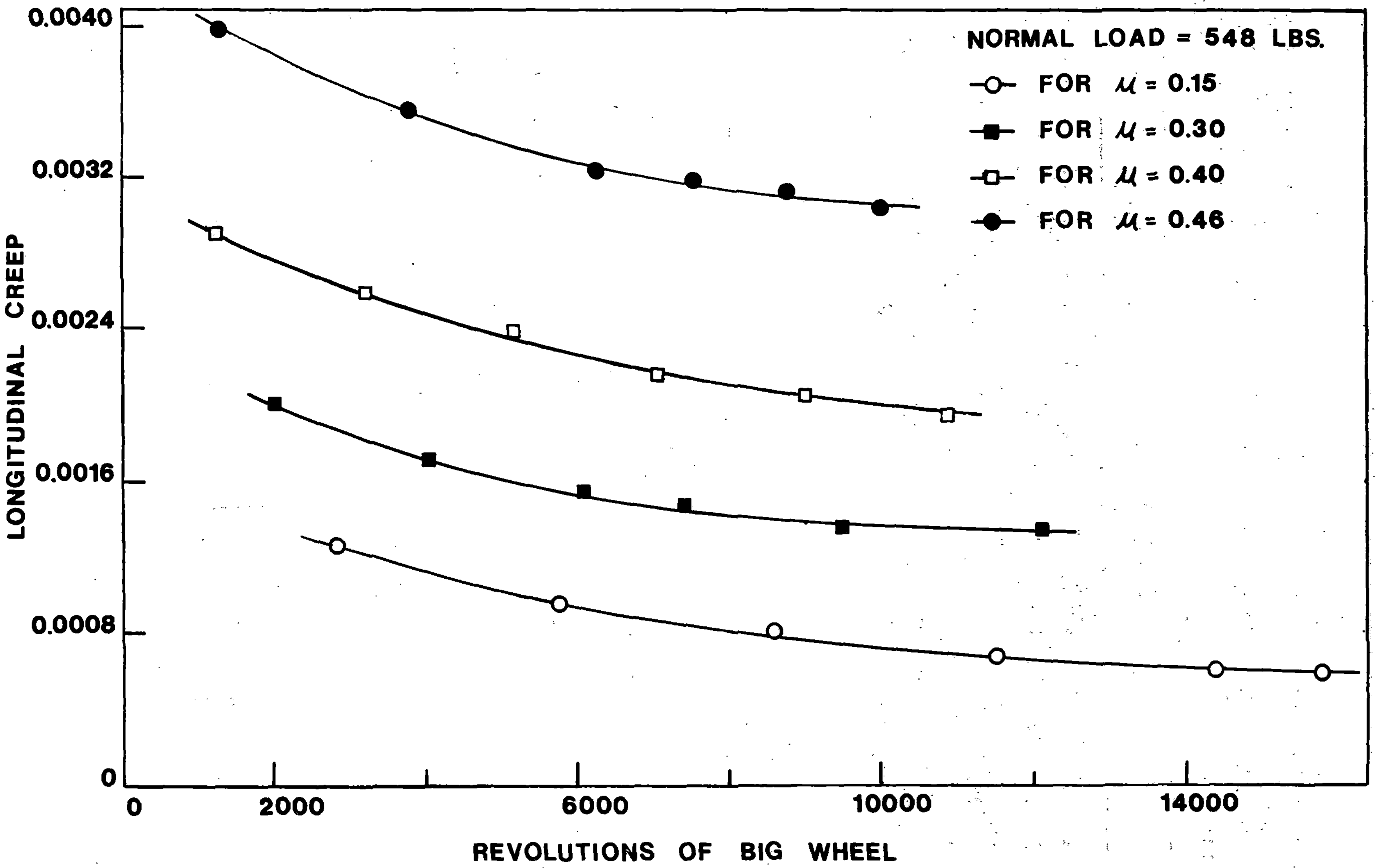

Figure 14. Longitudinal Creep vs. Revolutions of Big Wheel for Different Coefficients of Friction

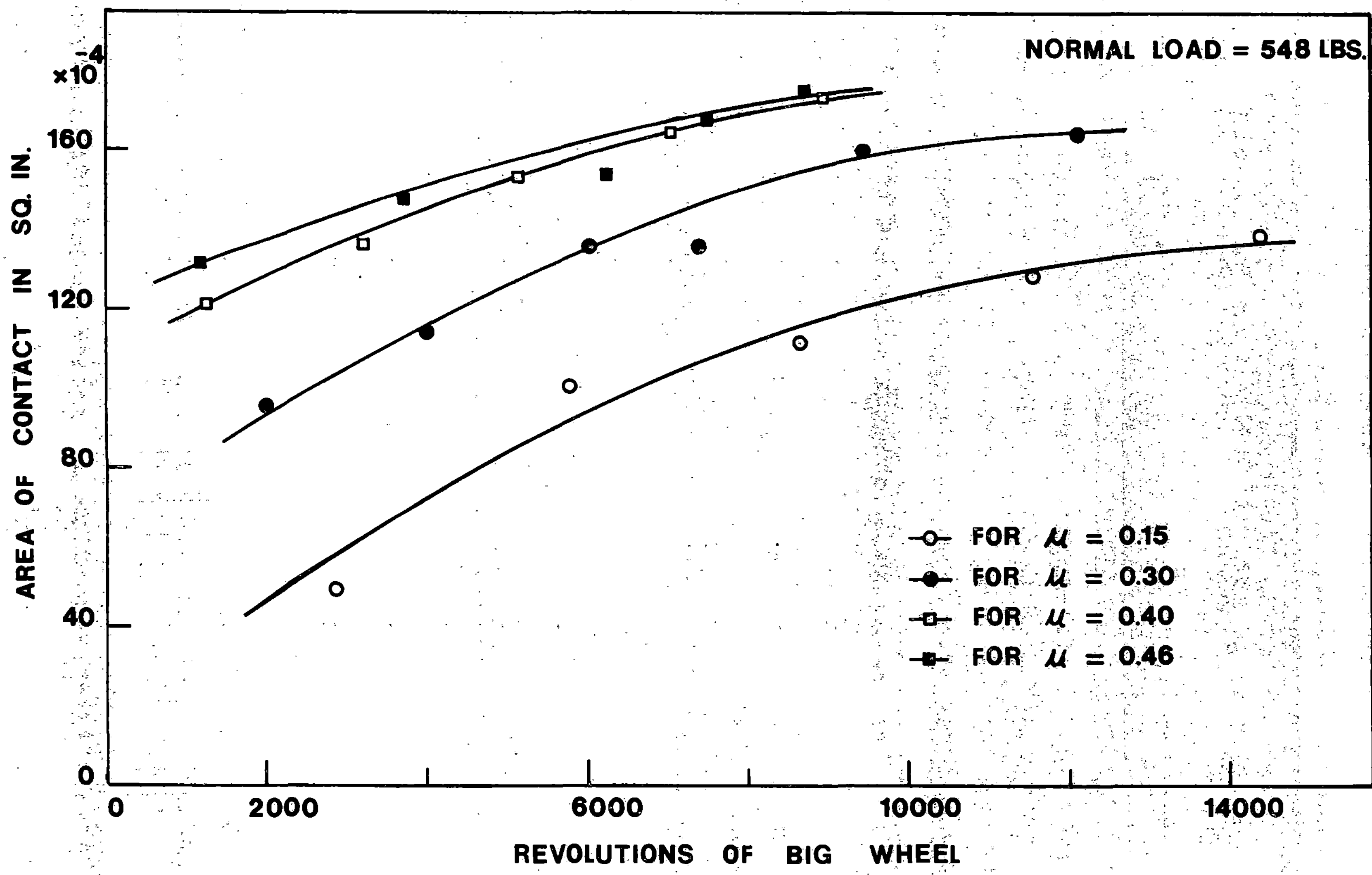

Figure 15. Area of Contact vs. Revolutions of Big Wheel for Different Coefficients of Friction

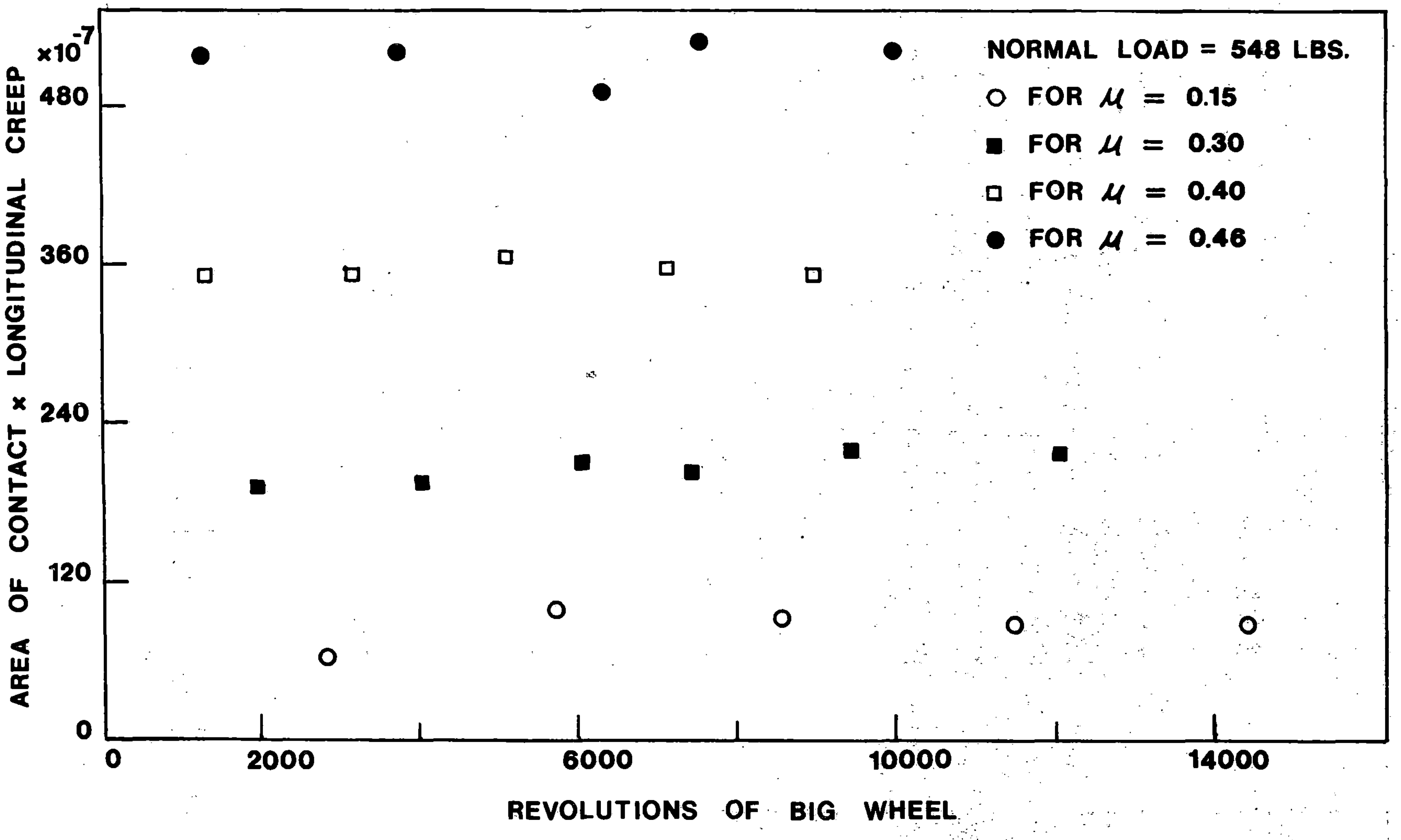

Figure 16. Product of Area Times Creep vs. Revolutions of Big Wheel for Different Coefficients of Friction

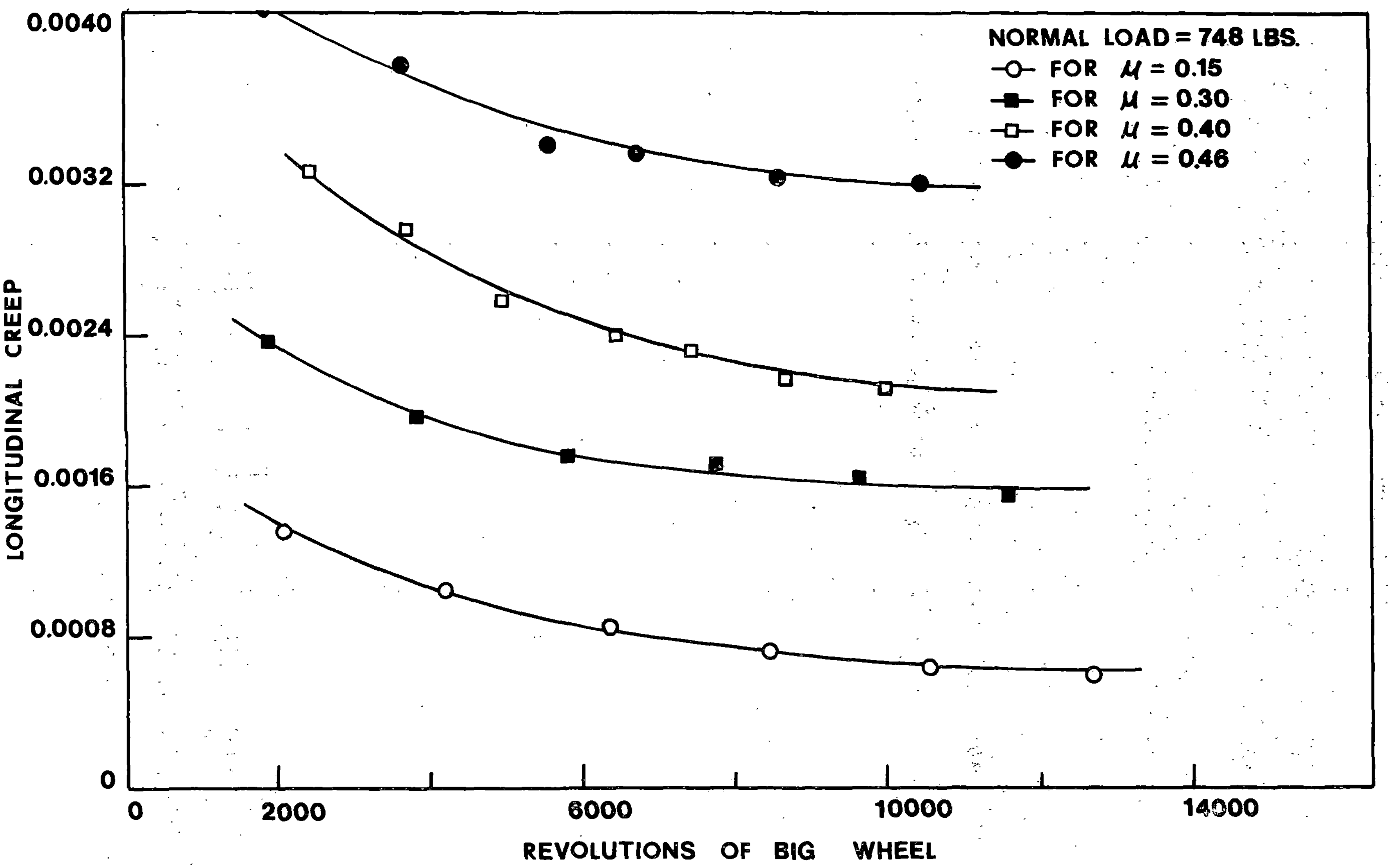

Figure 17. Longitudinal Creep vs. Revolutions of Big Wheel for Different Coefficient of Friction

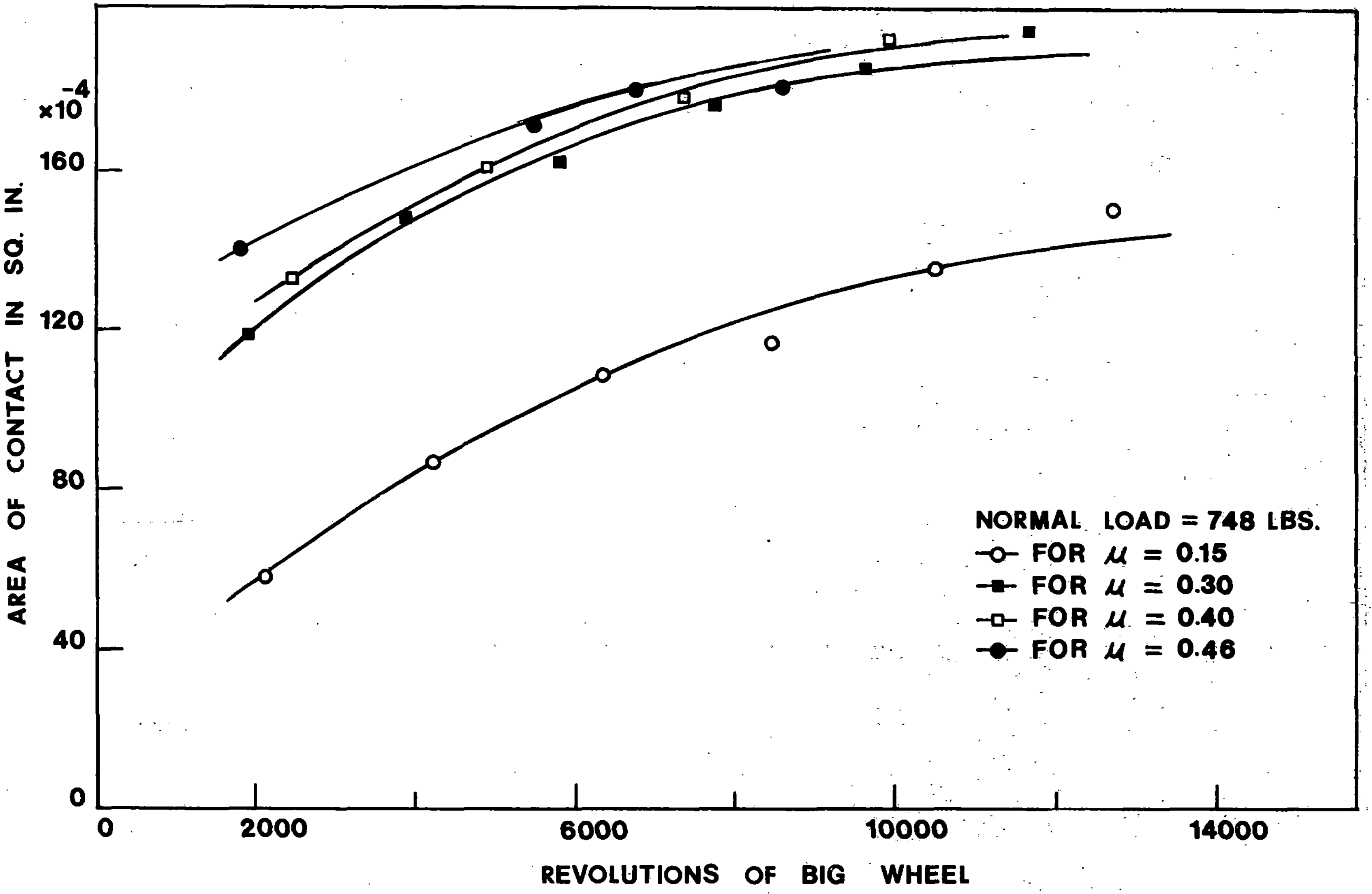

Figure 18. Area of Contact vs. Revolutions of Big Wheel for Different Coefficients of Friction

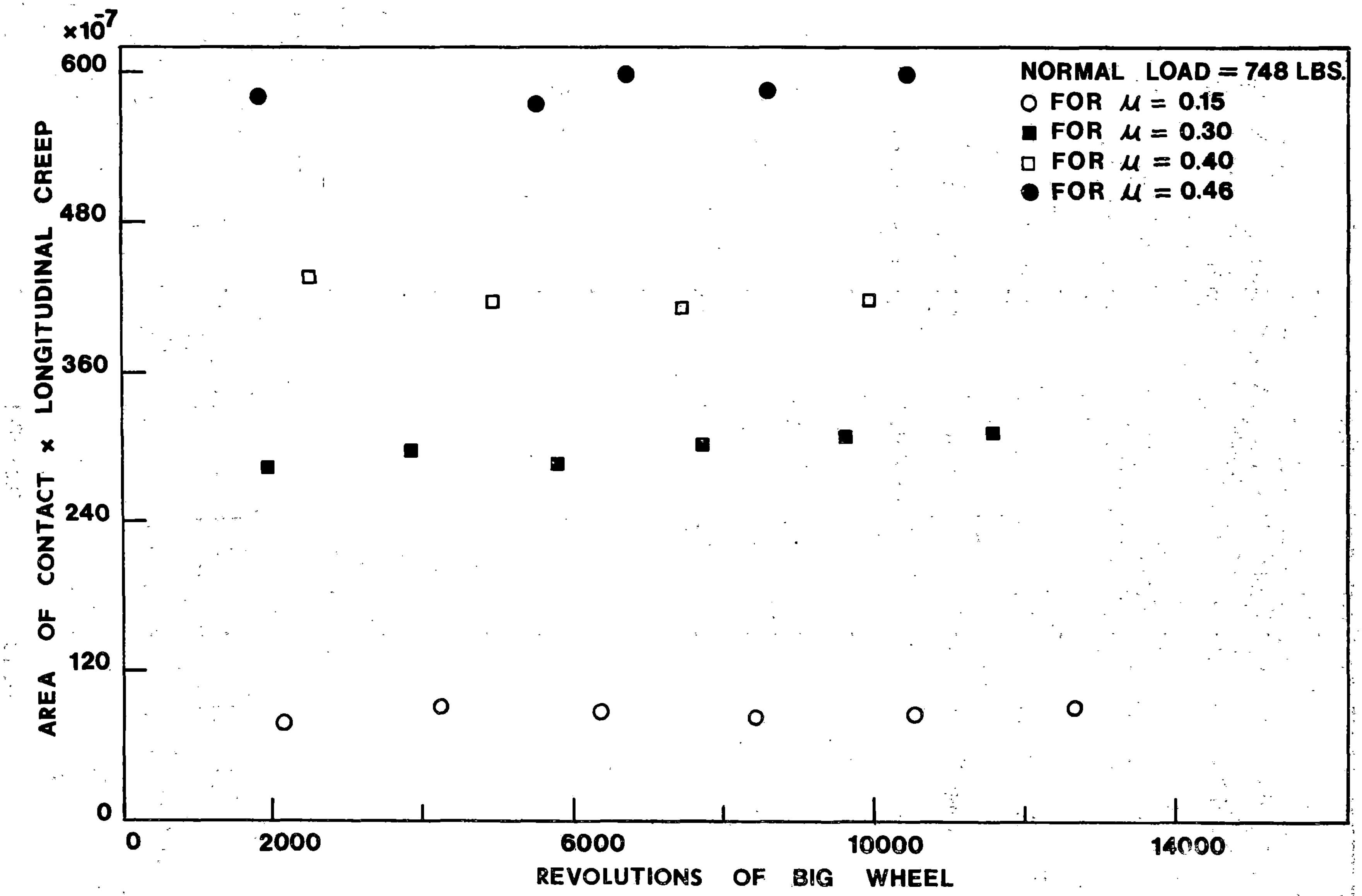

Figure 19. Product of Area Times Creep vs. Revolution of Big Wheel for Different Coefficients of Friction

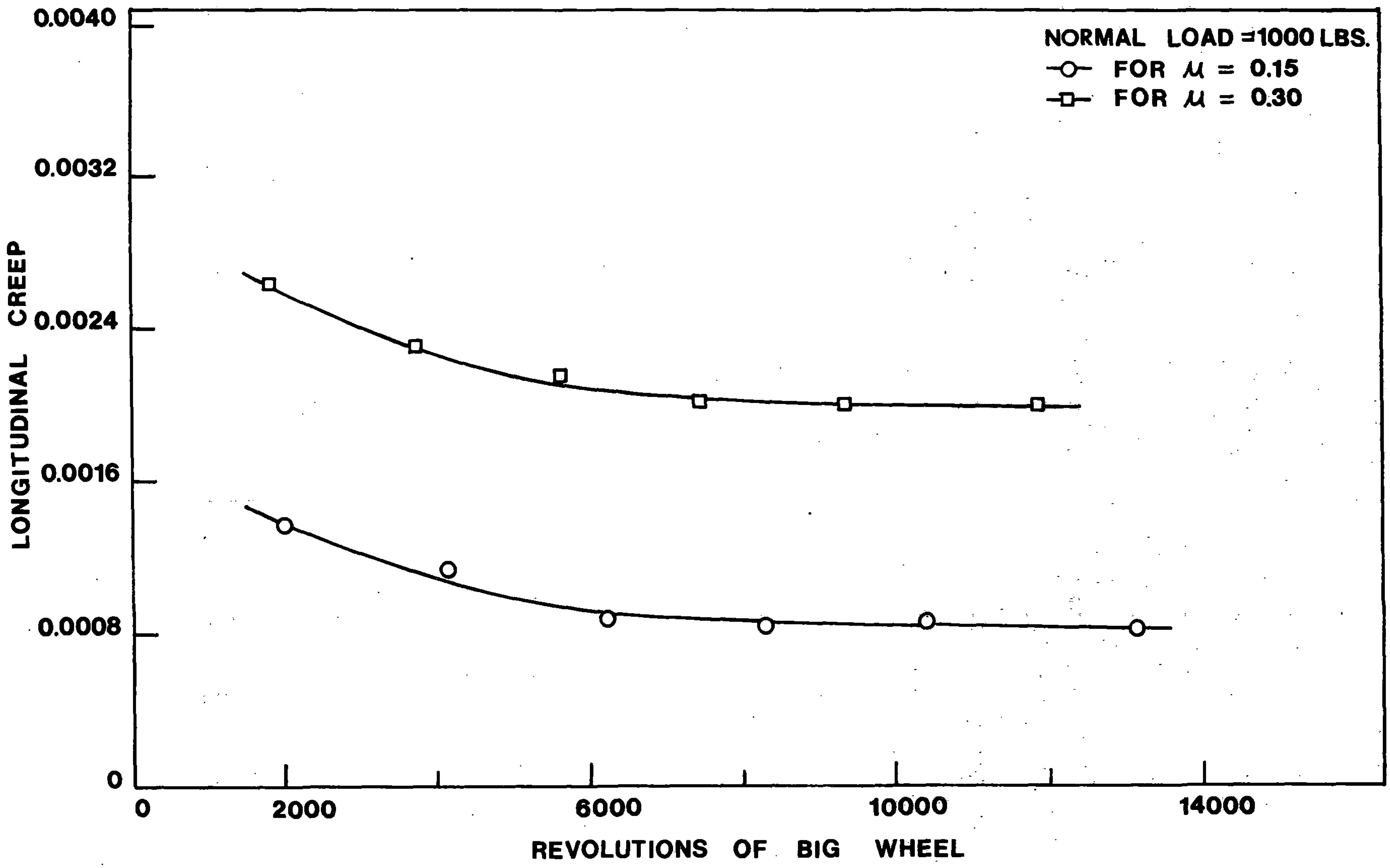

Figure 20. Longitudinal Creep vs. Revolutions of Big Wheel for Different Coefficients of Friction

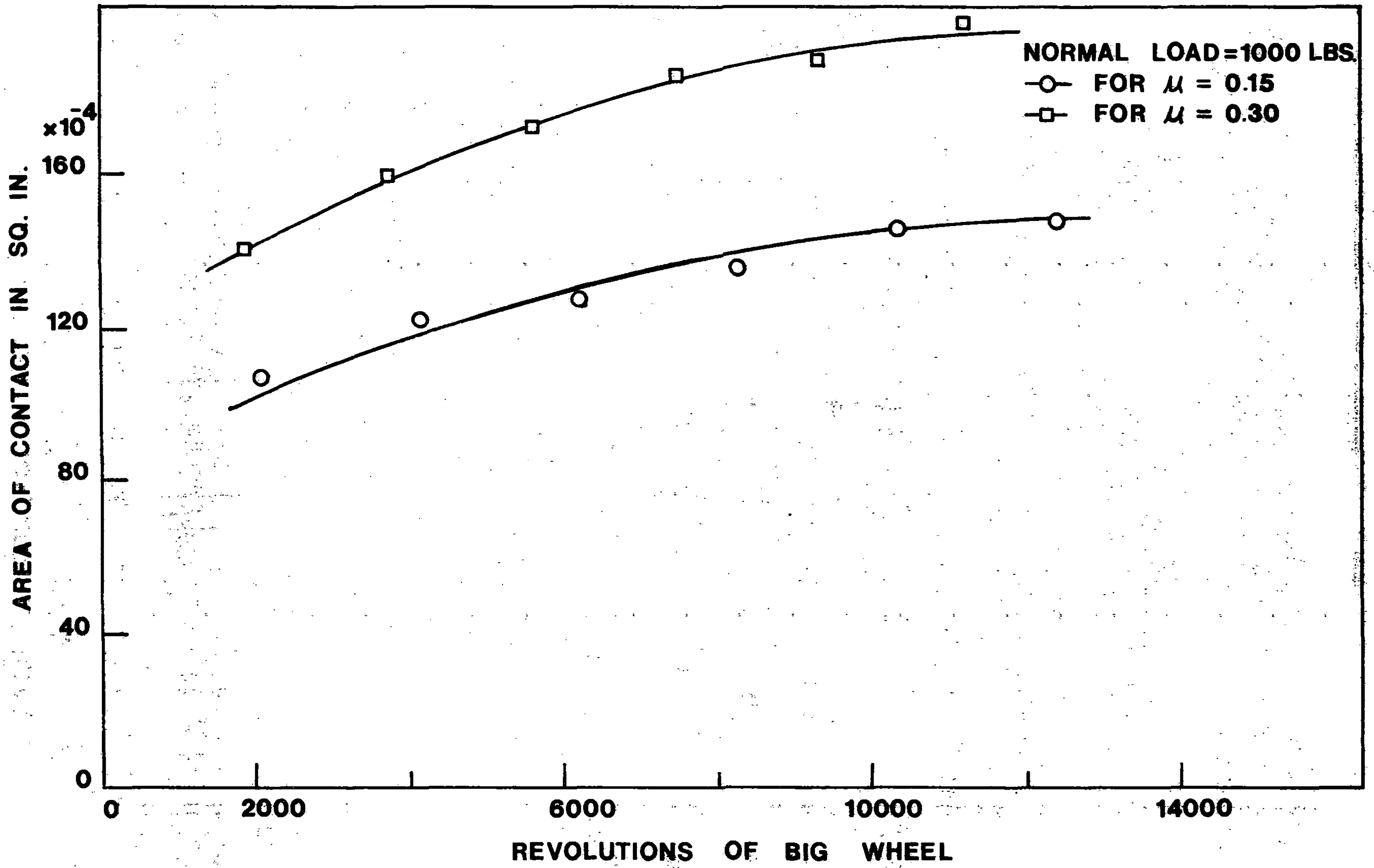

Figure 21. Area of Contact vs. Revolutions of Big Wheel for Different Coefficients of Friction

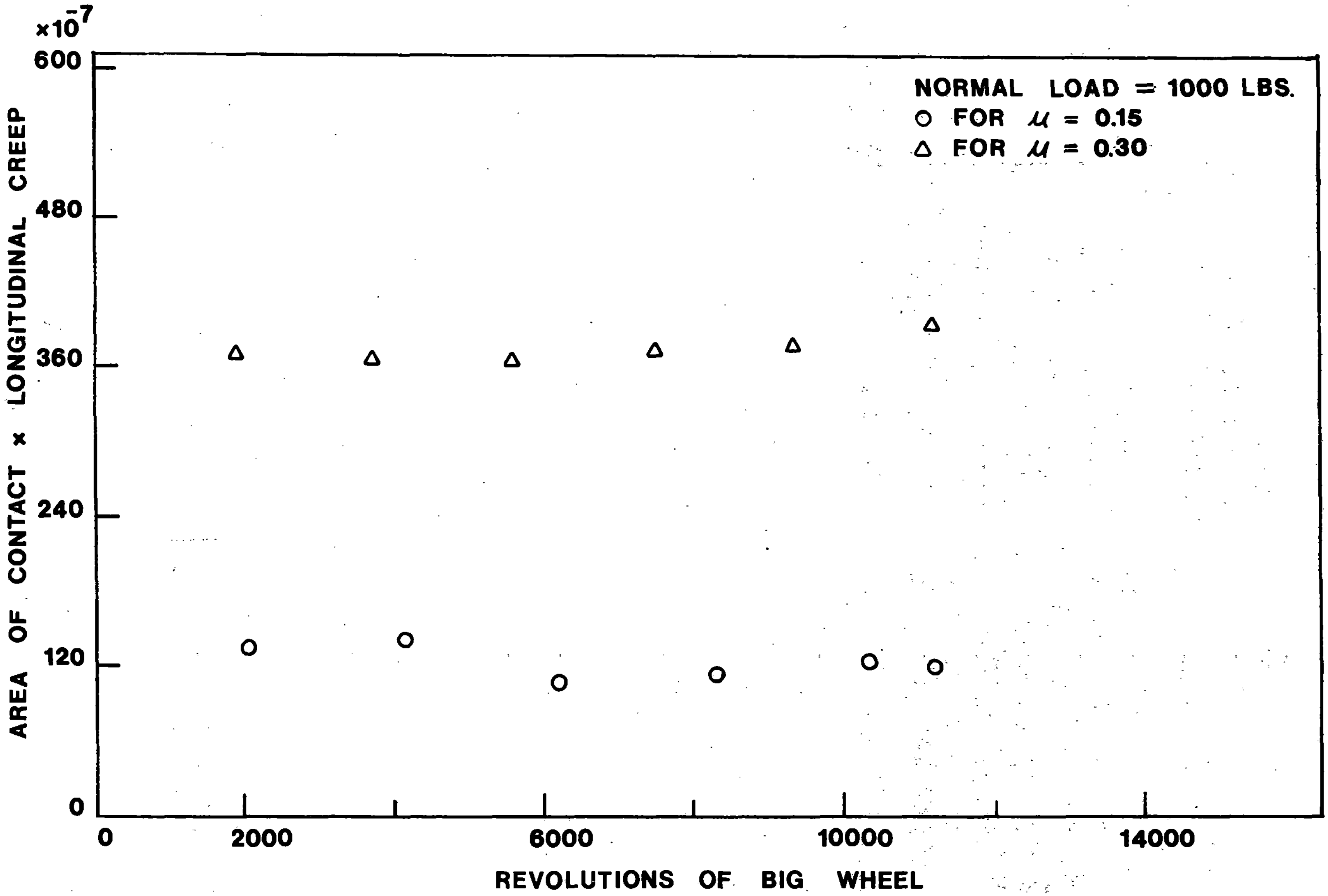

Figure 22. Product of Area Times Creep vs. Revolutions of Big Wheel for Different Coefficient of Friction

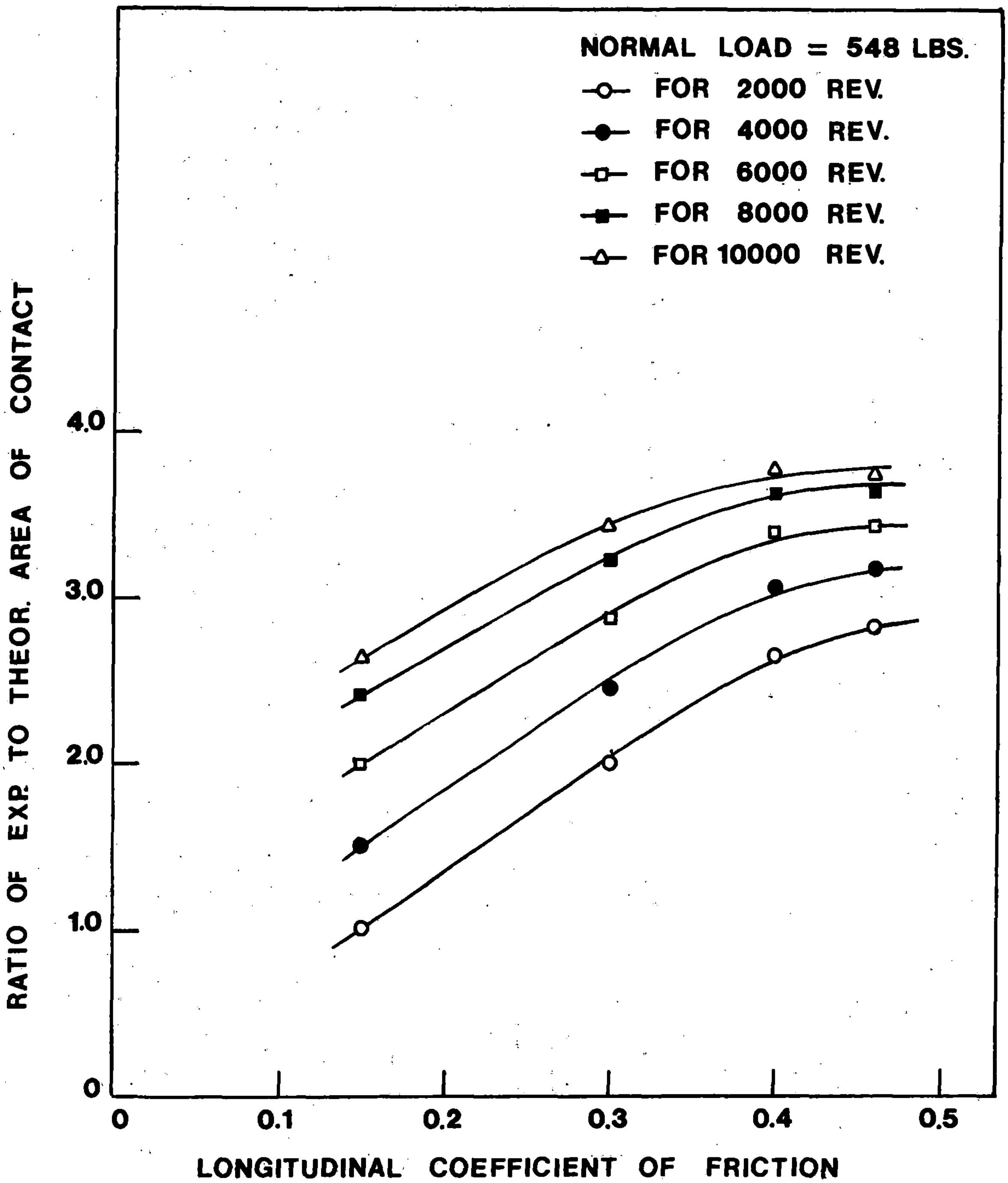

Figure 23. Ratio of Experimental to Theoretical Area of Contact vs. Longitudinal Coefficient of Friction

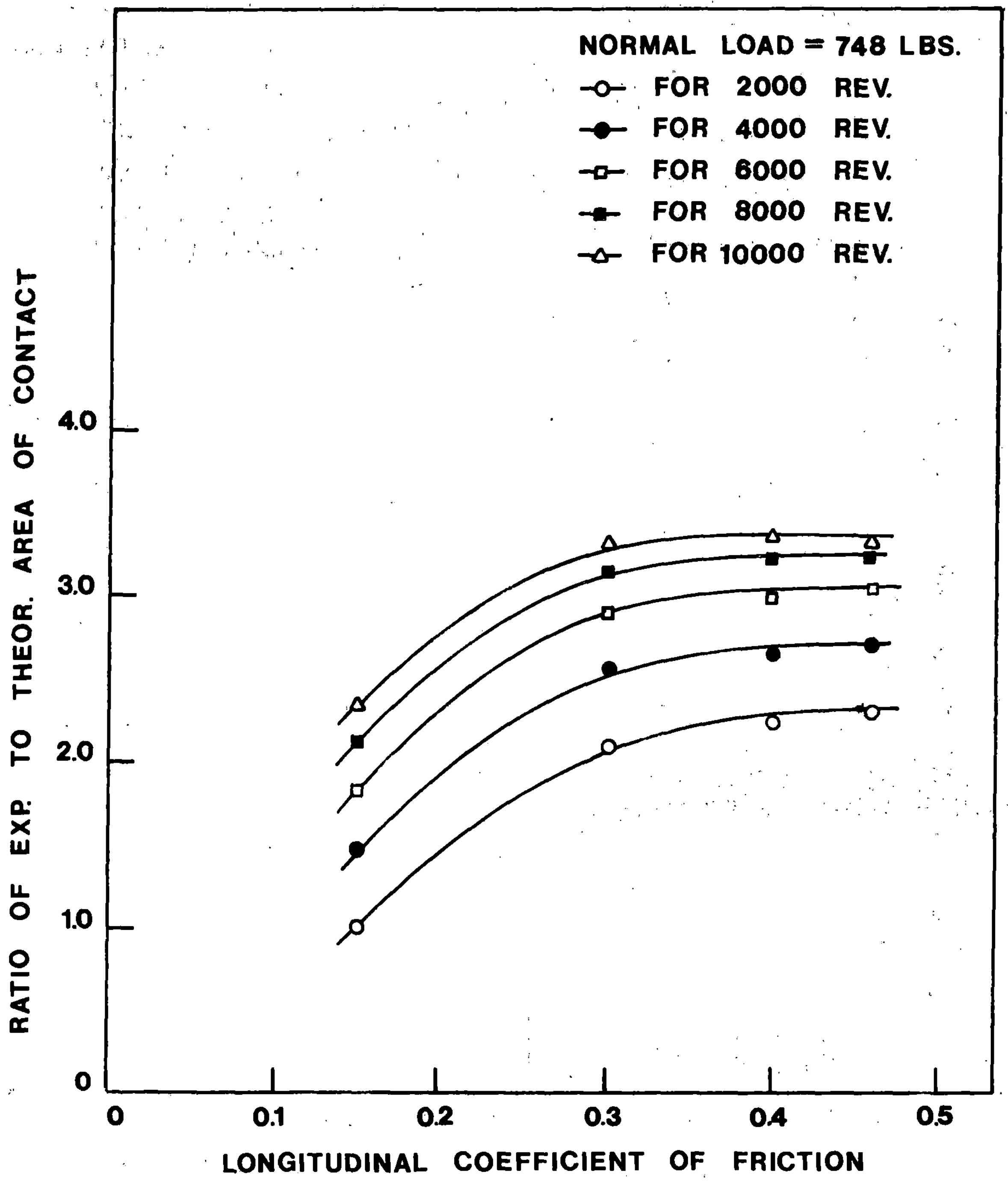

Figure 24. Ratio of Experimental to Theoretical Area of Contact vs. Longitudinal Coefficient of Friction

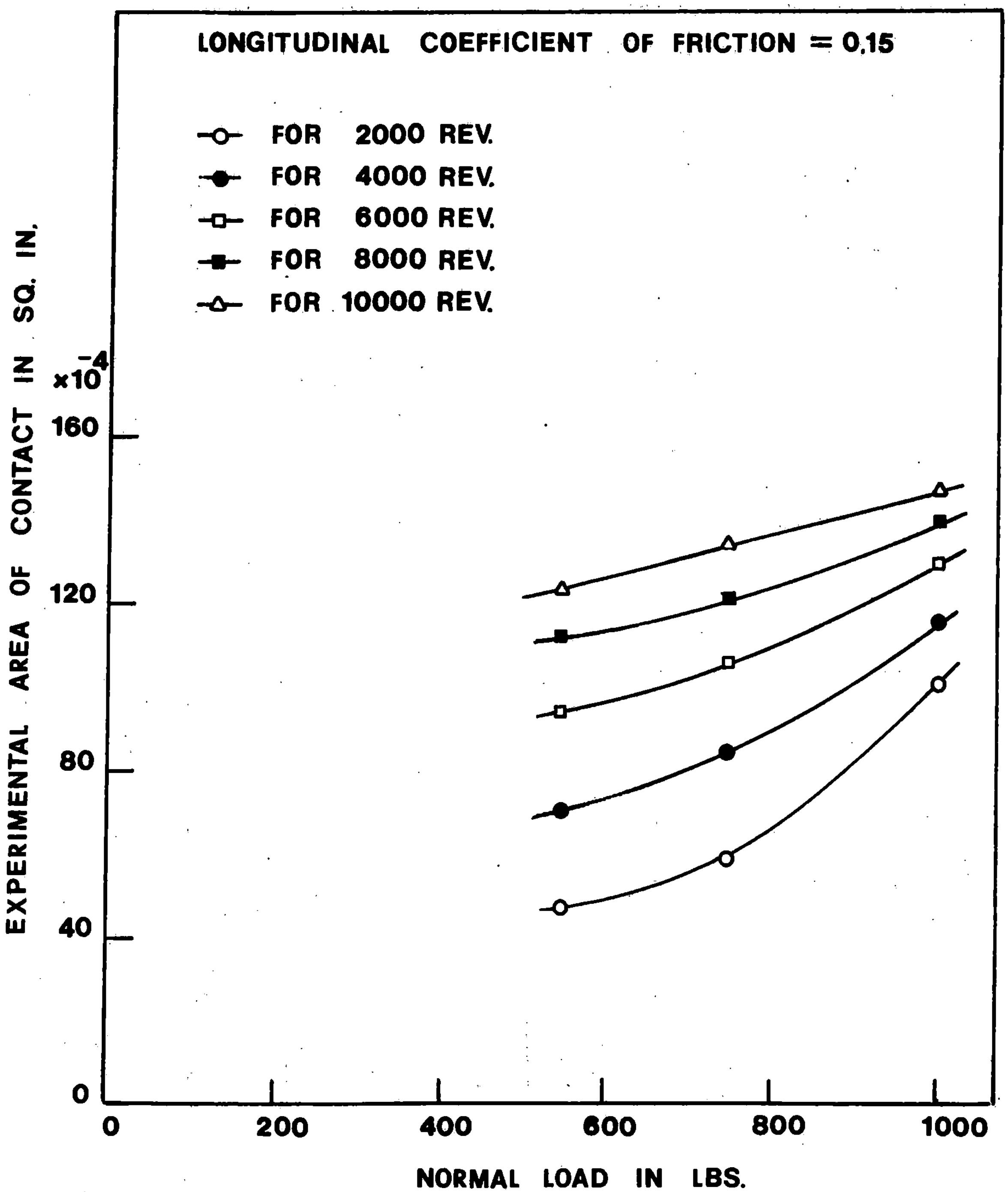

Figure 25. Experimental Area of Contact vs. Normal Load

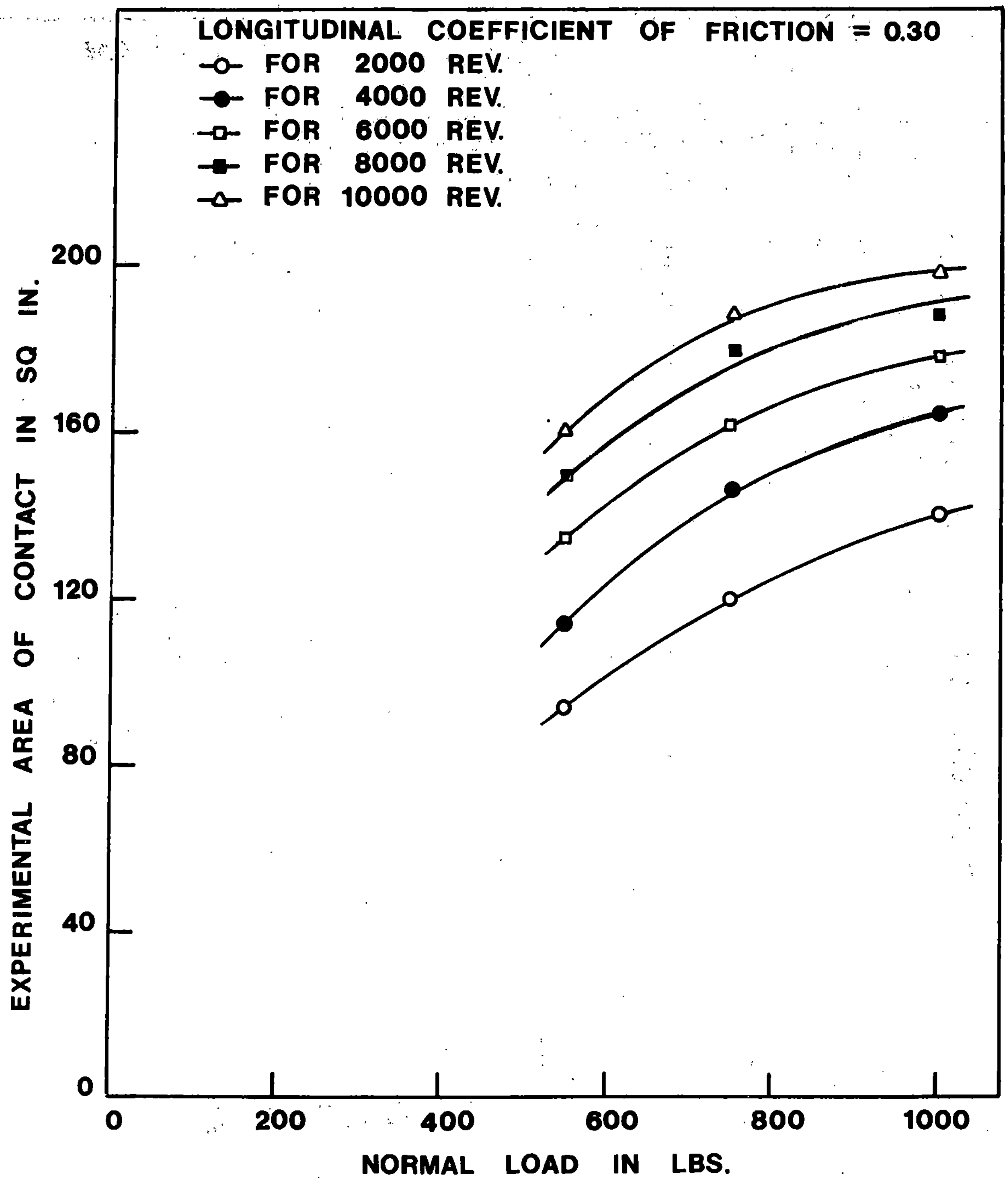

Figure 26. Experimental Area of Contact vs. Normal Load

V

CONCLUSIONS AND RECOMMENDATIONS

Discussion of Conclusions and Generalized Relations

The Friction-Creep Test Rig was designed to simulate road conditions in the laboratory. To duplicate the phenomena which occur in service, approximately the same Hertz contact stress level (200.000 psi), an elliptical contact area proportional to the actual and similar wheel and rail materials have been utilized for the tests. Under these stresses the wheels experience considerable wear as they roll. This wear takes place during the first hours of running and after this period the rate of wear is considerably reduced. As a consequence of the wear, the area of contact is changed from an ellipse to a rectangle, and for all practical purposes the equations corresponding to a cylindrical wheel can be applied. Not only the shape of the area of contact is changed but also the roughness of the surface is considerably increased due to the wear. The wear and roughness of the surface of contact have an important effect, that the value of the area of contact is increased as compared to the values predicted by the Hertz equation. The test wheels have been machined with a profile radius, and the process of wear has the effect of increasing the width of contact, since the wear produces a flattening of the contact face. That is, the width of the contact area is determined by the profile radius and the rate of wear. For each width one can apply the Hertz equation and compute the length of contact. The computed values are smaller than those measured experimentally, indicating the effect of wear and roughness on the contact area. For example for N = 748 lb. Table 9 shows the theoretical and the measured values of 2a, the length of contact area.

Table 9. Theoretical and Measured Values of Length of Contact Area for Various Coefficients

μ	$2a_T$ Theor.	$2a_m$ Measured	$\frac{a_m}{a_T}$
	in	in	-
.15	0.0890	0.100	1.12
.30	0.0794	0.119	1.50
.40	0.0794	0.120	1.53
.46	0.0787	0.1212	1.54

Since the roughness increases with the value of μ, the ratio $\frac{a_m}{a_T}$ increases with μ.

It is also observed that as the wear increases and the tangential forces are kept constant, the creep values decrease, but the product of the creep and the area of contact remains a constant, for each value of N and μ.

The law of constancy of the product of the area and creep can be theoretically deduced from the equations of Carter and Poritsky for the rolling of a cylinder. Carter and Poritsky(10) have shown that the strain in the adhesion region is given by

$$\varepsilon_x = \frac{4\mu_c N}{\pi E a^2 \ell} (1 - \nu^2)\ c \tag{1}$$

Where μ_c is the maximum coefficient of friction between the wheel and the rail, a is the semi-length of contact, ℓ the cylinder width, c is the length that defines the positioning of the adhesion region (Figure 27). Equation (1) can be transformed into

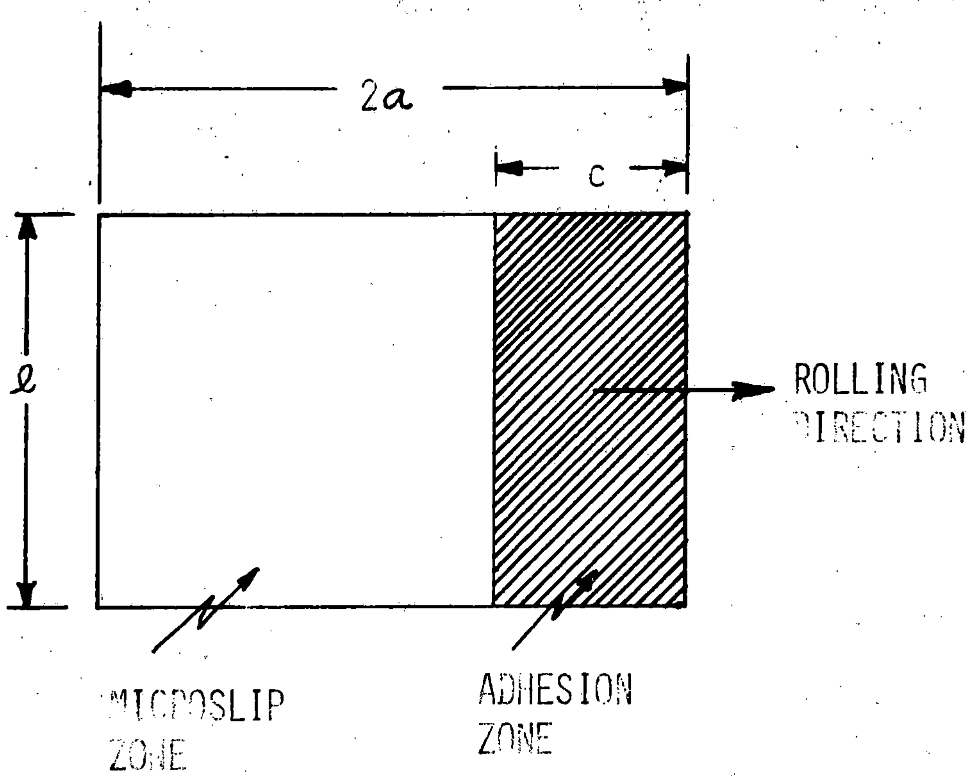

FIGURE 27. NOMENCLATURE FOR THE RECTANGULAR CONTACT ZONE OF A WORN WHEEL AND RAIL.

$$\varepsilon_x = \frac{8\mu_c N}{\pi E a A_c} (1-\nu^2)\ a \tag{2}$$

where

$$A_c = 2a\ell \tag{3}$$

Carter and Poritsky have also shown that

$$\frac{a}{c} = \sqrt{1 - \frac{T}{\mu_c N}} \tag{4}$$

where T is the traction force.
Therefore we can obtain the equation

$$\varepsilon_x = \frac{8\mu_c N}{\pi E A_c} (1 - \nu^2) \left[1 - \sqrt{1 - \frac{T}{\mu_c N}} \right] \tag{5}$$

Carter and Poritsky have also shown that the relative velocities V_S of the two surfaces in contact are

$$V_S = V_{avg} (\xi + 2\ \varepsilon_x) \tag{6}$$

where $V_{avg} = \frac{V_1 + V_2}{2}$ is the average of the velocities of the two surfaces in contact.

For the stick zone $V_S = 0$ and

$$\xi = 2\varepsilon_x \tag{7}$$

consequently from Eq. (5) we obtain

$$\xi\ A_c = \frac{16\mu_c N}{\pi E} (1 - \nu^2) \left[1 - \sqrt{1 - \frac{\mu}{\mu_c}} \right] \tag{8}$$

where T has been replaced by μN.

We can see that the produce ξA_c remains constant for given values of μ_c, N, and μ. μ_c is itself a function of N, as it is shown in Figure 28 where the values of μ_c obtained from the tests utilized to obtain

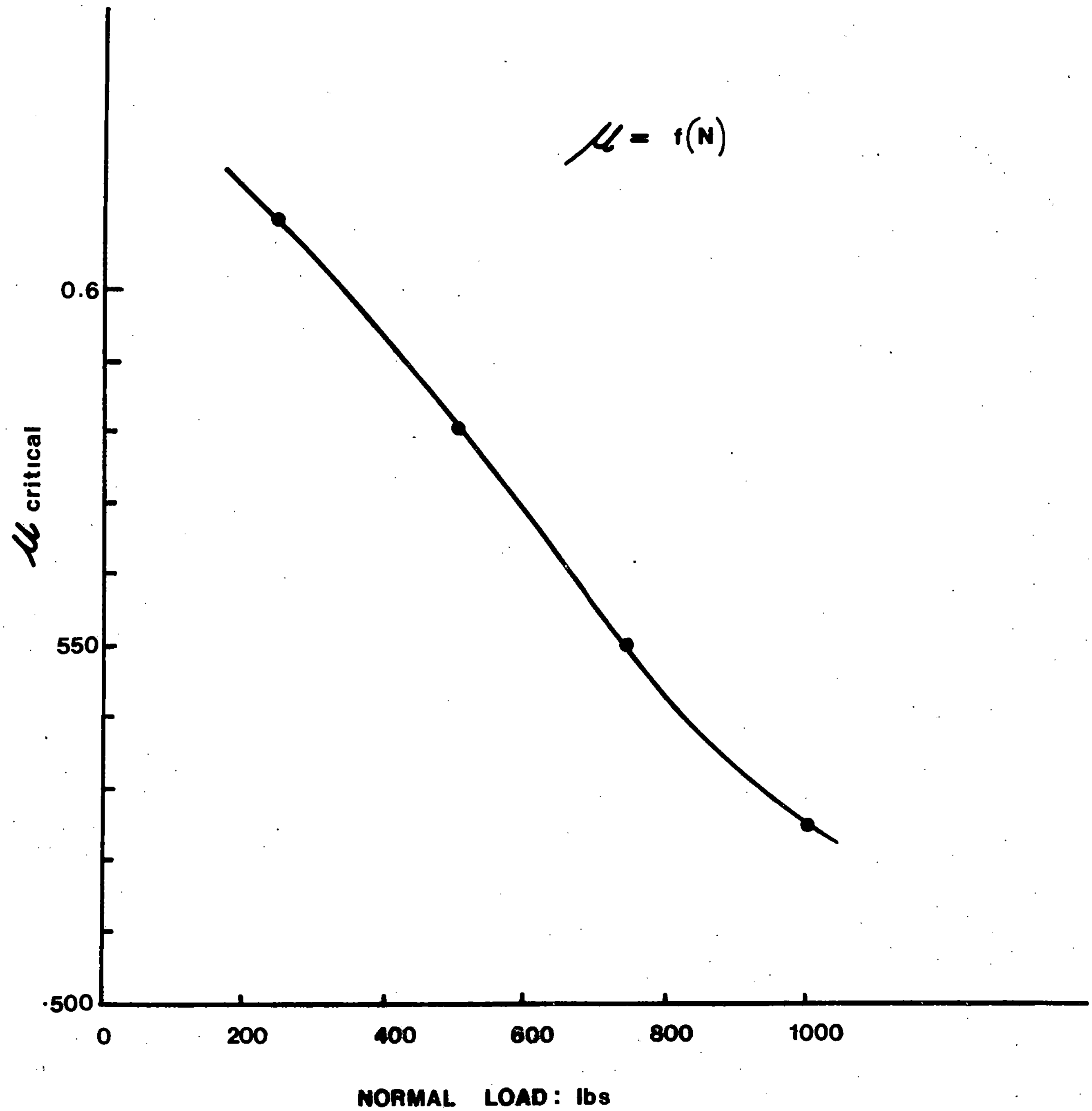

FIGURE 28. $\mu_{CRITICAL}$ AS A FUNCTION OF THE NORMAL LOAD N.

the curves of ξ **versus** μ have been plotted. Consequently, the product of ξA_c is a function of μ and N. The tests carried out at constant values of μ provide us the necessary information to see if the Carter-Poritsky equation (8) is satisfied. From Eq. (8) we can write

$$k = \frac{\xi A_c}{\mu_c N \left(1 - \sqrt{1 - \frac{\mu}{\mu_c}}\right)} \doteq \frac{16\,(1 - \nu)^2}{\pi E} = 1.5645 \times 10^{-7} \quad (9)$$

Computations were carried out for the experimental values and the following table was obtained:

Table 10. Ratio k of Equation 10 for Various μ and N.

N / μ	548 lb. $k \times 10^7$	748 lb. $k \times 10^7$	1000 lb. $k \times 10^7$	$10^7 \times k$ avg
0.15	1.892	1.73	1.625	1.75
0.30	2.090	2.21	2.089	2.13
0.40	2.493	2.142	-	2.29
46	2.906	2.248	-	2.61

We can see that the ratio k depends strongly on μ. The influence of N is not as clear because we do not have enough data. It may be neglected as compared to the influence of μ. If we plot on a log paper k versus μ, the points fall on a straight line of slope 1/3, Figure 29. Taking into consideration this observation the ξA_c relation can be expressed

$$\xi A_c = 3.28 \times 10^{-7}\, \mu^{\frac{1}{3}}\, \mu_c N \left[1 - \sqrt{1 - \frac{\mu}{\mu_c}}\right] \quad (10)$$

$$\xi A_c = 3{\cdot}28\times10^{-7}\,\mu^{1/3}\mu_c N\left[1-\sqrt{1-\frac{\mu}{\mu_c}}\right]$$

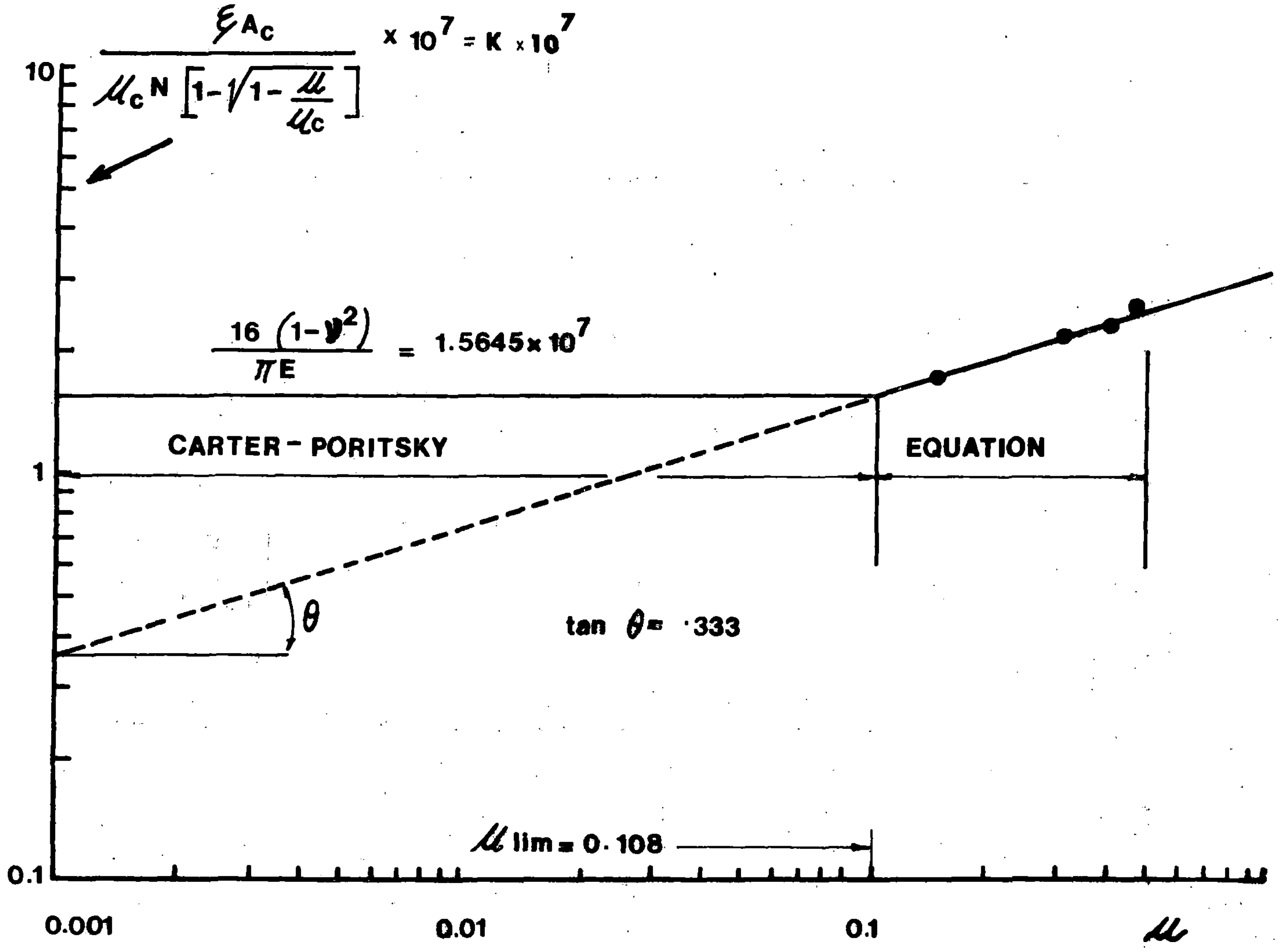

FIGURE 29. LOG-LOG PLOT OF $\kappa \times 10^7$ VS. μ SHOWING CARTER-PORITSKY EQUATION TOGETHER WITH EXPERIMENTAL RESULTS AND THE PLOT OF EQUATION (10).

Equation (10) gives the Carter-Poritsky results for μ_{lim} = 0.108.

To verify the validity of this equation one can go back to results obtained in the initial group of tests and see if the equation can predict the values of the creep versus friction coefficient curve.

Figure 30 shows the experimental values plotted together with the values predicted by Equation (10). Figure 30 also shows the values given by an empirical equation of the form

$$\xi A_c = 0.558 \frac{\mu N}{\mu_c} \frac{10^{-7}}{\left[1 - \left(\frac{\mu}{\mu_c}\right)^2\right]^{\frac{1}{2}}} \qquad (11)$$

values. The computations were repeated for the time corresponding to the stabilization of the contact areas, that is for t $\geqslant$ 270 minutes. In this case the agreement is very close, (Fig. 31). In the same figure the values predicted by the Carter-Poritsky equation have been plotted. Since the Carter-Poritsky equation predicts areas of contact smaller than the measured areas, and therefore the values of creep given by the equation are larger than the measured values.

In the same figure the points corresponding to the dimensionless curve of Fig. 11 are plotted. This curve averages all the results corresponding to the measured ξ versus μ curves, and agrees extremely well with the values corresponding to the Kalker's solution. It is possible to see that the values predicted by Equation (10) almost coincide with the values corresponding to the dimensionless curve. We can reduce Equation (10) to the form

$$\frac{G\ \xi\ A_c}{\pi\ \mu_c\ N} = \frac{G \times 3.28}{\pi} \times 10^{-2}\ \mu^{\frac{1}{3}} \left[1 - \sqrt{1 - \frac{\mu}{\mu_c}}\right] \qquad (12)$$

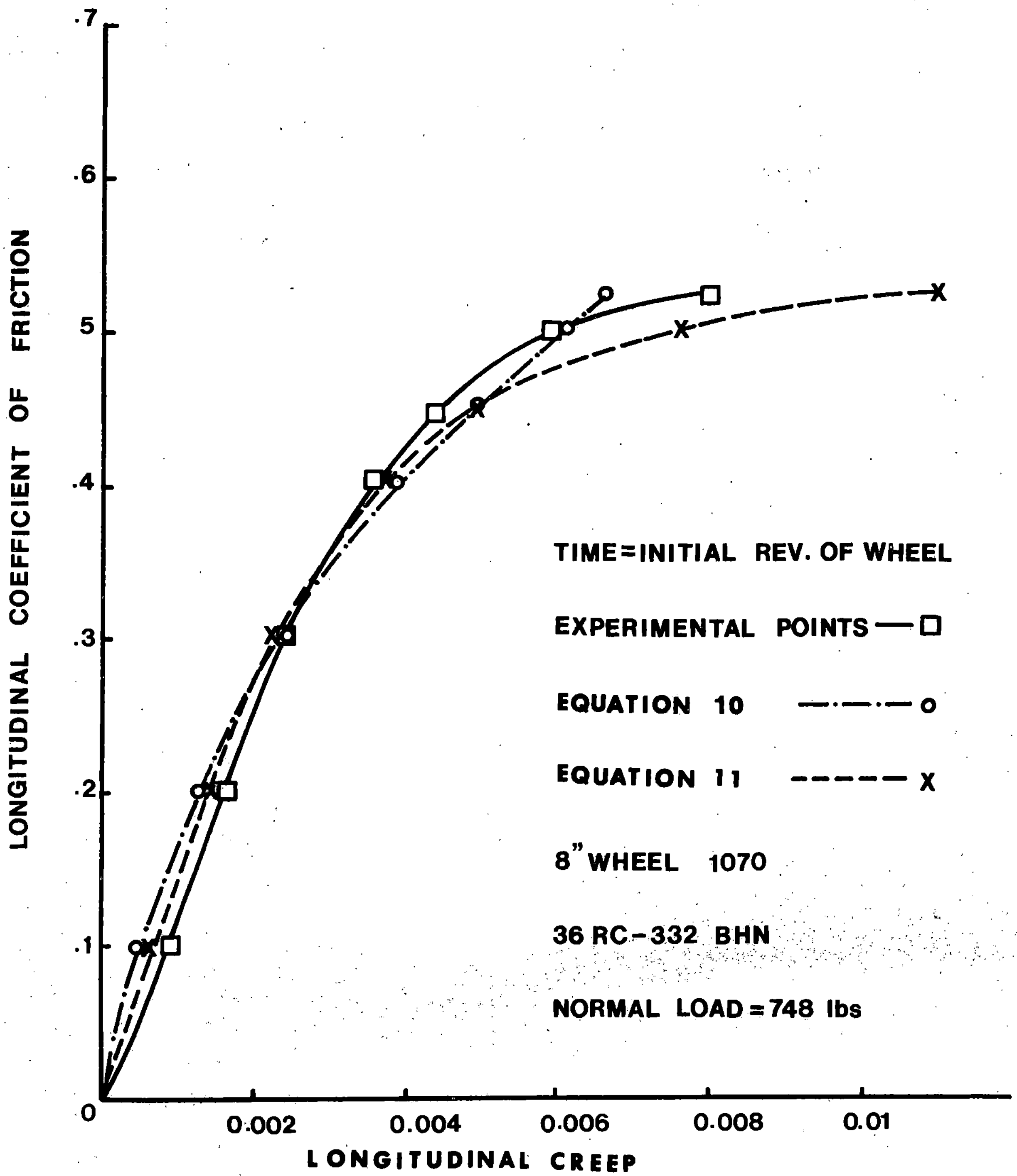

FIGURE 30. ADHESION VS. CREEP CURVE FOR SMOOTH SURFACE, EXPERIMENTAL VALUES AND VALUES PREDICTED BY ANALYTICAL EXPRESSIONS.

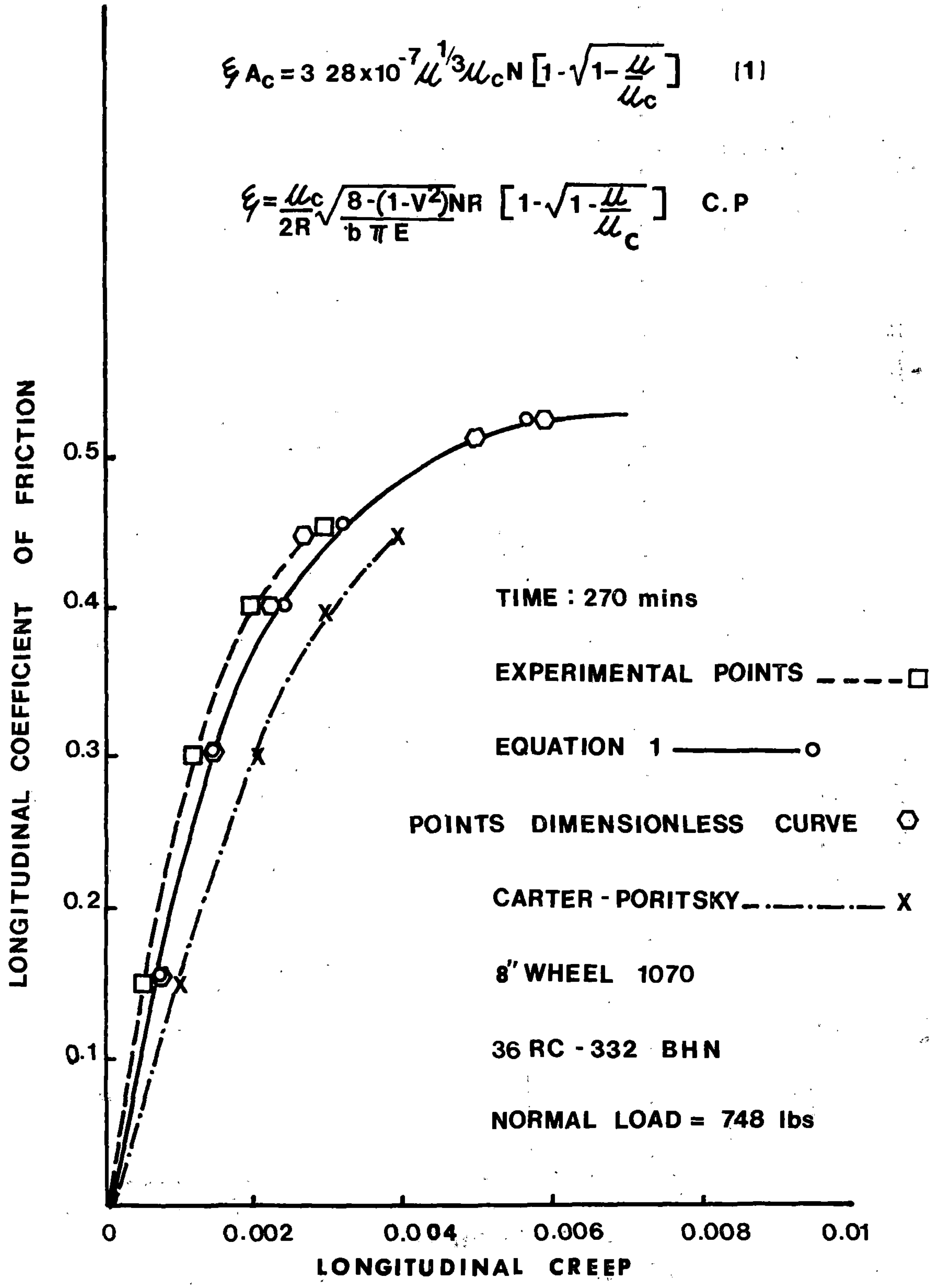

FIGURE 31. ADHESION VS. CREEP CURVE FOR A WORN OUT SURFACE. EXPERIMENTAL VALUES AND VALUES PREDICTED BY ANALYTICAL EXPRESSIONS.

If the number 3.28 is practically approximated with π, we get

$$\frac{G \xi A_c}{\pi \xi_c N} = G \times 10^{-7} \mu^{\frac{1}{3}} \left[1 - \sqrt{1 - \frac{\mu}{\mu_c}}\right] \tag{13}$$

For steel the above equation takes the form

$$\frac{G \xi A_c}{\pi \mu_c N} = 1.13 \mu^{\frac{1}{3}} \left[1 - \sqrt{1 - \frac{\mu}{\mu_c}}\right] \tag{14}$$

Plotting the results of Equation (14) with the average values given by Tables 1 to 4, we can see an almost perfect agreement, Figure 32. A simpler expression can be obtained if the μ_c factor is eliminated and only the operating friction coefficient μ and the normal load N are included in consideration. For such a case, the experimental data fits with the following relation:

$$\frac{A \xi}{\mu^{1.56} N} \times 10^7 = 2.52 \tag{15}$$

This relation is plotted in Figure 33. It holds for the railroad track and wheel steels used in the laboratory tests. For other steels, it is felt that the constant on the right hand side will change. Tests with other materials are needed before the material properties can be included in this equation. Constancy of $(A \xi G)/\mu^{1.56} N$ is, however, suspected.

We can see that the whole of the results presented in this report can be summarized by Equations (14) and (15). These equations seem to be valud under very general conditions. They are valid at the initial rolling period where there are very high stresses, and very intense wear, and continue to be valid after the surfaces of contact have become rough, the area of contact has

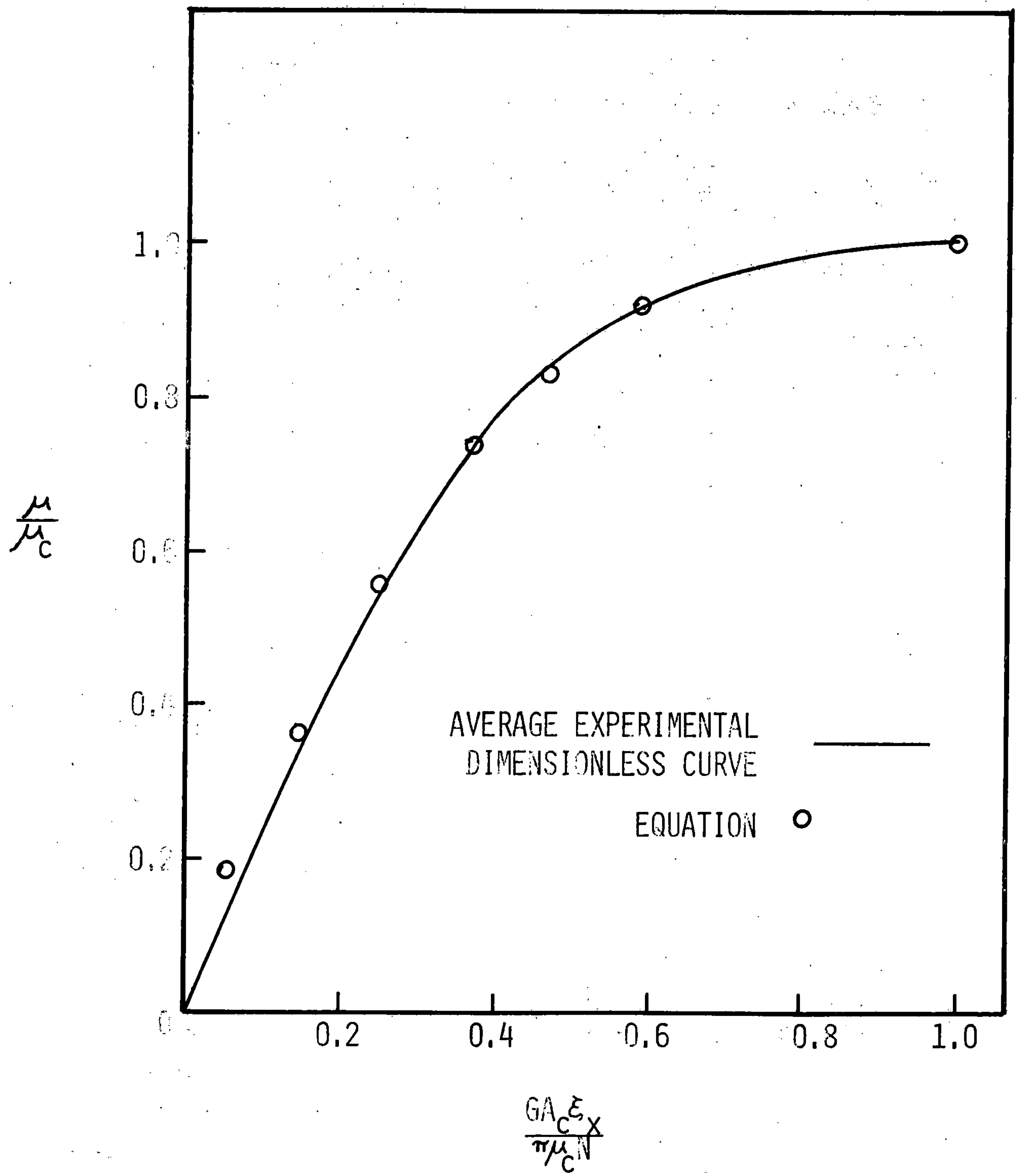

FIGURE 32. DIMENSIONLESS ADHESION VS. CREEP CURVE. AVERAGE EXPERIMENTAL VALUES AND VALUES PREDICTED BY EQUATION (13).

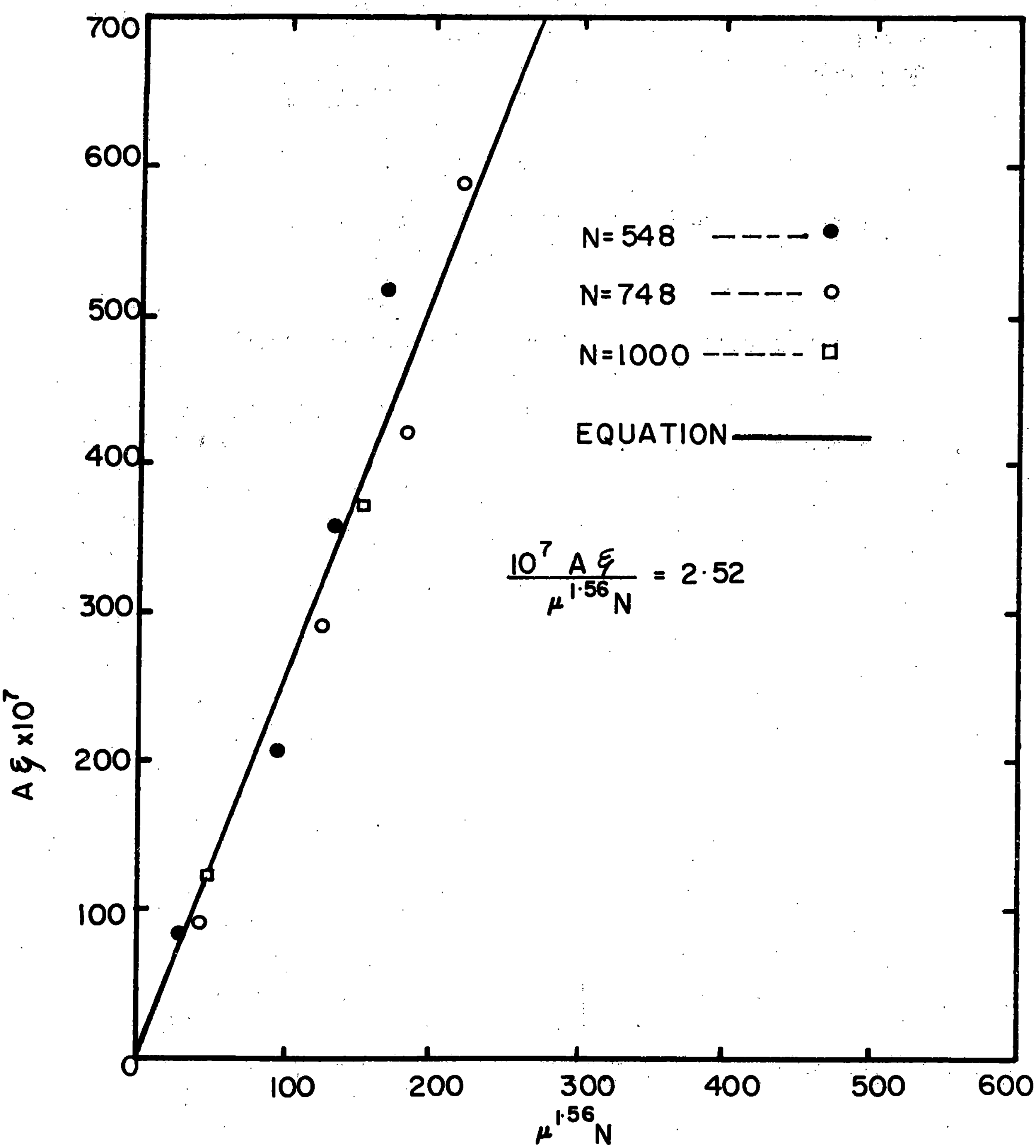

FIGURE 33. SIMPLIFIED GENERAL RELATION BETWEEN ACTUAL AREA OF CONTACT, CREEP, FRICTION COEFFICIENT AND NORMAL LOAD FOR SMOOTH AND ROUGH SURFACES.

increased and the stresses have been considerably reduced. During this period the shape of the contact area has changed from elliptical to rectangular.

Recommendations for Designs to Improve Locomotive Traction

From Equations (14) and (15), it can be seen that the amount of creep for a given value of μ can be reduced by increasing the contact area. High creep means high strains since both are directly connected. In turn high strains imply a larger wear. Consequently for a given tractive effort it is beneficial to have as large an area of contact as feasible. This calls for a change of the profiles of rails and wheels to obtain a large area of contact. As it is not readily possible to change the profile of rails, a change in wheel profile and design is recommended. Use of steels with high shear modulus should also provide the solution of good traction with low wear. Further work in these directions is recommended.

APPENDIX A

SUMMARY OF CALCULATIONS

Simulation of Road Condition

The ratio of the major axis to the minor axis of the ellipse of contact between a G.M. EMD locomotive wheel and rail is 1.57. In order to simulate load conditions, it was desired that the contact between the big and the small wheel used for experimentation be an ellipse, the ratio of the major to minor axis of which is 1.57. In order to achieve this, the profile of the small wheel was given a curvature, the radius of which is calculated in the following manner.

Following are the symbols and their meaning needed for the understanding of the subsequent equations.

N	=	normal load
a, b	=	semi-major and semi-minor axis of the contact area
$\frac{1}{r_3}, \frac{1}{r_4}$	=	principal curvatures of the large wheel at the point of contact
$\frac{1}{r_1}, \frac{1}{r_2}$	=	principal curvatures of the small wheel
ϕ	=	angle between the normal planes containing curvatures γ_2 and γ_3 at the point of contact (Figure 28)
E	=	modulus of elasticity
Y	=	Poisson's ratio

Modulus of elasticity and Poisson's ratio of both the wheels are the same.

The semi-axis of the ellipse of contact are given by:[8]

$$a = \alpha \sqrt[3]{\frac{Nm}{n}} \qquad b = \beta \sqrt[3]{\frac{Nm}{n}}$$

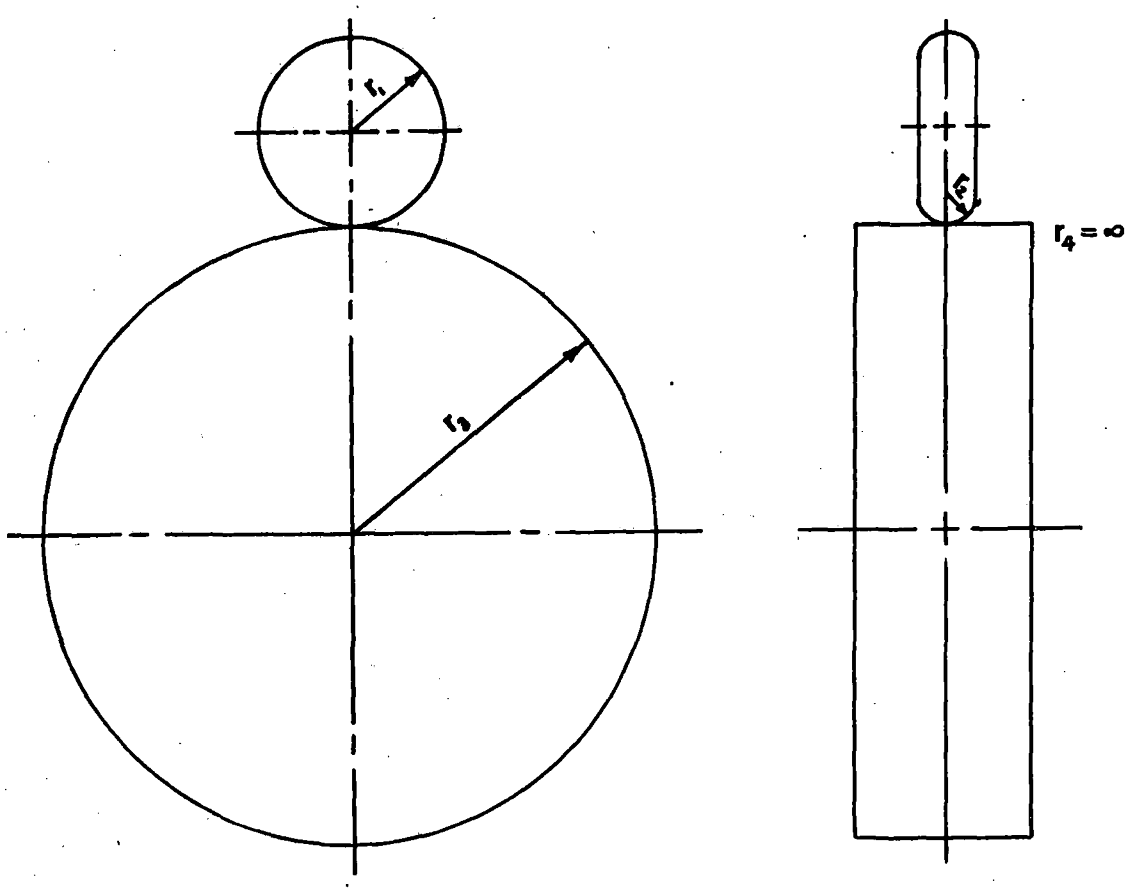

Figure 34. Two Normal Planes Containing Curvatures r_2 and r_3 Perpendicular to Each Other at the Point of Contact

where

$$m = \frac{4}{\frac{1}{r_1} + \frac{1}{r_2} + \frac{1}{r_3} + \frac{1}{r_4}}$$

and

$$n = \frac{4E}{3(1 - \quad ^2)}$$

but a = 1.57 b (due to simulation needs).

Therefore:

$$\alpha \sqrt[3]{\frac{Nm}{n}} = 1.57 \quad \beta \sqrt[3]{\frac{Nm}{n}}$$

or

$$\alpha = 1.57 \beta.$$

From Figure 29:

$$\alpha = 1.27, \beta = .81, \text{ and } \theta = 71^o$$

where θ is defined as

$$\cos \theta = \frac{B}{A} = .32557,$$

or

$$B = .32557 A.$$

where

$$A = \frac{2}{m} = \frac{2}{\frac{4}{\frac{1}{r_1} + \frac{1}{r_2} + \frac{1}{r_3} + \frac{1}{r_4}}}$$

but $r_4 = \infty$

Hence, $A = \frac{1}{2} \quad \frac{r_2 r_3 + r_1 r_3 + r_1 r_2}{r_1 r_2 r_3}$

and $B = \frac{1}{2} \sqrt{(\frac{1}{r_2})^2 + (\frac{1}{r_2} - \frac{1}{r_3})^2 + 2 \; (\frac{1}{r_1})(\frac{1}{r_2} - \frac{1}{r_3}) \cos 2\phi}$

where

$$\phi = 90^o .$$

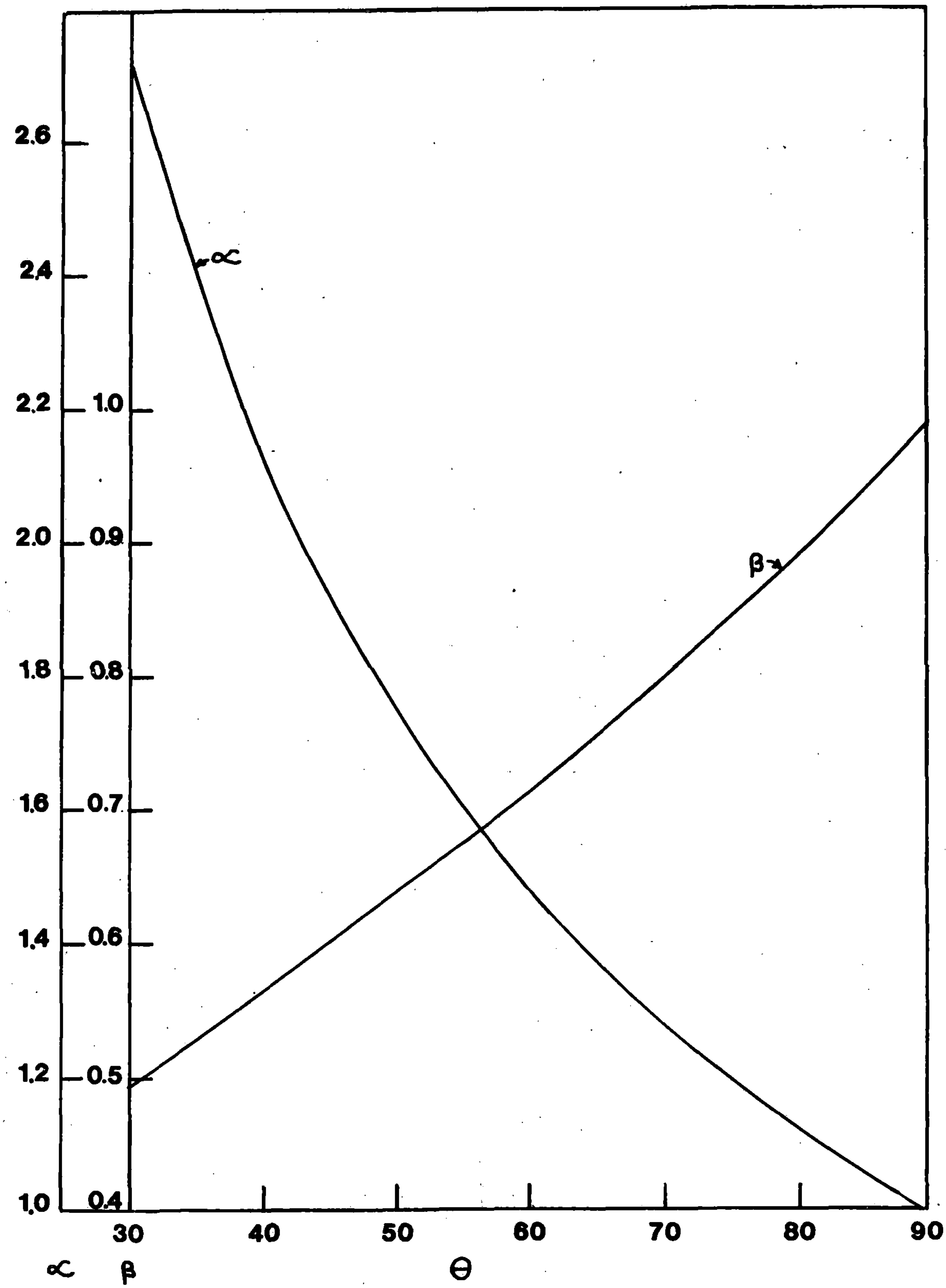

Figure 35. α and β Used for Calculation of Semi-Axis of the Ellipse of Contact

Now,

$$B = .32557\ A$$

or

$$B = (.32557)^2\ A$$

or

$$B^2 = K^2\ A^2$$

so;

$$\left(\frac{1}{r_1}\right)^2 + \left(\frac{1}{r_2} - \frac{1}{r_3}\right)^2 + 2\left(\frac{1}{r_1}\right)\left(\frac{1}{r_2} - \frac{1}{r_3}\right)(-1)$$

$$= K \times \frac{r_2^2 r_3^2 + r_1^2 r_3^2 + r_1{}^2 r_2{}^2 + 2r_3^2 r_1 r_2 + 2r_2^2 r_1 r_3 + 2r_1^2 r_2 r_3}{r_1^2 r_2^2 r_3^2}$$

or

$$\frac{r_2^2 r_3^2 + r_1^2 r_3^2 - 2r_1^2 r_2 r_3 - 2r_3^2 r_1 r_2 + 2r_2^2 r_1 r_3 + r_1^2 r_2^2}{r_1^2 r_2^2 r_3^2} =$$

$$\frac{Kr_2^2 r_3^2 + Kr_1^2 r_3^2 + Kr_1^2 r_2^2 + 2Kr_3^2 r_1 r_2 + 2Kr_2^2 r_1 r_3 + 2Kr_1^2 r_2 r_3}{r_1^2 \quad r_2^2 \quad r_3^2}$$

or

$$r_2^2\ (r_3^2 + 2r_1 r_3 + r_1^2 - Kr_3^2 - Kr_1^2 - 2Kr_1 r_3)$$

$$+ r_2(-2r_1{}^2 r_3 - 2r_3^2 r_1 - 2Kr_3^2 r_1 - 2Kr_1^2 r_3)$$

$$+ (r_1^2 r_3^2 - Kr_1^2 r_3^2) = 0.$$

The above equation may be written as:

$$ar_2^2 + br_2 + c = 0,$$

where:

$$a = r_3^2 + 2r_1 r_3 + r_1^2 - Kr_3^2 - Kr_1^2 - 2Kr_1 r_3\ ,$$

$$b = + -2r_1{}^2 r_3 - 2r_3^2 r_1 - 2Kr_3^2 r_1 - 2Kr_1^2 r_3$$

$$c = + r_1^2 r_3^2 - Kr_1^2 r_3^2 = 0.$$

Now, $r_1 = 4$ and $r_3 = 17.696$.

Substituting these values of r_1 and r_3, we get:

$a = 420.822$
$b = 3397.021$
$c = 4479.296$

and the above equation becomes -

$$420.822r_2^2 - 3397.021r_2 + 4479.296 = 0.$$

Hence,

$$r_2 = \frac{3397.021 + \quad (-3397.021)^2 - 4(420.822)(4479.296)}{841.6649}$$

or

$$r_2 = \frac{3397.021 + 1999.9494}{841.6449}$$

or

$$r_2 = 1.659929.$$

Hence, the profile radius on the small wheel = 1.660.

<u>Calculation of the Semi-Major and Semi-Minor Axis of Ellipse of Contact for Normal Load = 548 lb.</u>

$$a = \alpha \sqrt[3]{\frac{Nm}{n}}$$

or $$a^3 = \alpha^3 \frac{Nm}{n}$$

Now,

$$n = \frac{4E}{3(1 - \quad ^2)} = \frac{4 \times 30 \times 10^6}{3\ (1 - (0.3)^2} = \frac{1.20 \times 10^8}{2.73} = 4.395 \times 10^7$$

$$m = \frac{4}{\frac{1}{4} + \frac{1}{1.66} + \frac{1}{17.696} + \frac{1}{\ }} = \frac{4}{.9089} = 4.40092$$

Therefore,

$$a^3 = \frac{2.04838 \times 548 \times 4.40092}{4.395 \times 10^7} = .000112402$$

or

$$a = 0.04830$$

and $$b = \frac{0.04830}{1.57} = .030764$$

Hence, theoretical area of contact = 0.0046657.

8" Wheel With Profile Radius = 1.660"

Load, in lbs.	Semi-Major Axis "a" in inches	Semi-Minor Axis "b" in inches	Area of Contact in Square Inches
248	0.0370	0.02356	0.0027372
548	0.0483	0.03076	0.0046657
748	0.0535	0.03408	0.0057287
1000	0.0590	0.03757	0.0069602

<u>Calculation of error due to reduction in diameters of the two wheels with wear.</u>

The change in diameter of the small wheel when the rig was operating at 1000 lb. and .3 coefficient of friction for 5 hours was observed to be 0.0006".

With reference to I.I.T. interim technical report [2].

$$\nu = \frac{R_S}{R_B}$$

$$\therefore \quad d\nu = -\frac{R_S}{(R_B)^2}\, dR_B + \frac{dR_S}{R_B}$$

Now,

$$R_S = \frac{7.9172}{2} = 3.9586"$$

$$R_B = \frac{35.392}{2} = 17.696"$$

$$dR_S = 0.0003"$$

$$dR_B = 0.0003" \text{ (assumed to be approximately same)}$$

Hence

$$d_\nu = \frac{39586}{(17.696)^2} \times 0.0003 + \frac{0.0003}{17.696}$$

or

$$d\nu = -.0000037 + .0000169$$

$$d\nu = 0.0000132$$

The change in longitudinal creep $d\xi_x$ is written as [2] $d\xi_x$

$$= -d\nu \frac{N_S}{N_B} + \nu \frac{N_S}{N_B^2} dN_B - \frac{\nu}{N_B} dN_S$$

$$\therefore \quad d\xi_x = -0.0000132 \times \frac{442.6}{99.2} + 0 + 0$$

$$\therefore \quad d\xi_x = 0.0000588$$

Hence the maximum error introduced in the creep readings by not taking the change in diameter into account is 0.0000588 which is very small. The value of N_S and N_B are taken when the rig is operating at 1000 lb. normal load and · 3 coefficient of friction for 5 hours.

APPENDIX B

EXPERIMENTAL TEST DATA

For Figure 2. Longitudinal Run

8" Wheel, Plain 1070, 36 RC
Vertical Load - 248 lbs
Area of Contact - .0050895 Sq. In.

SR NO.	Frequency From Big Wheel N_B (C/S)	Frequency From Small Wheel N_S (C/S)	Longitudinal Strain Gauge Reading (μin/in)	N_S / N_B	Longitudinal Creep	Longitudinal Coefficient in Friction
1	121.7	541.2	5	4.44700	.0006005	.0122189
2	121.3	539.8	30	4.450123	.0001012	.0733187
3	121.4	539.7	30	4.445634	.0009077	.073137
4	120.7	536.7	50	4.4465617	.0006992	.1221895
5	120.6	536.2	50	4.446102	.0008024	.1221895
6	119.4	530.5	80	4.4430485	.0014888	.1955032
7	119.6	530.0	80	4.431438	.0040890	.1955032
8	118.4	525.4	110	4.43750	.0027357	.2688169
9	118.3	525.4	110	4.4412510	.0018927	.2688169
10	118.3	525.5	110	4.442096	.0017028	.2688169
11	117.1	520.3	160	4.4432109	.0014523	.3421306
12	117.3	520.7	140	4.4390451	.002388512	.3421306
13	117.2	520.4	180	4.4402730	.00211257	.3421306
14	115.9	514.0	180	4.434857	.00332960	.4398822
15	115.9	514.1	210	4.4357204	.00313519	.4398822
16	115.9	509.3	210	4.428695	.0034570	.5131959
17	114.9	509.5	210	4.4392906	.00404379	.5131959
18	114.9	509.2	210	4.4316797	.00404379	.5131959
19	114.1	504.0	240	4.4171179	.007302866	.5865096
20	113.9	503.8	240	4.4131782	.00595438	.5865096

← Slippage at 260

For Figure 3. Longitudinal Run

8" Wheel, plain 1070, 36 R.C.
Vertical Load - 498 lbs
Area of Contact - .008935 Sq. In.

SR NO.	Frequency From Big Wheel N_B (C/S)	Frequency From Small Wheel N_S (C/S)	Longitudinal Strain Gauge Reading (μ in/in)	N_S/N_B	Longitudinal Creep	Longitudinal Coefficient of Friction
1	120.6	536.3	30	4.446932	.00061606	.0365096
2	120.7	536.9	30	4.448218	.00032689	.0365096
3	119.3	530.2	60	4.444258	.00121696	.0730192
4	119.2	529.7	60	4.4437919	.00132174	.0730192
5	117.6	522.7	90	4.444727	.00111406	.1095289
6	117.8	523.4	90	4.4431239	.00147187	.1095289
7	124.4	552.9	120	4.444533	.001155033	.1460385
8	124.5	553.6	120	4.446586	.00069374	.1460385
9	124.5	553.0	120	4.4417670	.00177680	.1460385
10	123.3	547.8	150	4.4428223	.0015396	.1825481
11	123.2	547.9	150	4.447240	.00054678	.1825481
12	123.3	548.5	150	4.4484995	.0002637	.1825481
13	122.0	542.5	185	4.4426229	.0015844	.2251427
14	122.2	542.8	185	4.4418985	.00174726	.2251427
15	121.0	537.7	210	4.4438016	.00131956	.255676
16	121.2	538.0	210	4.4389438	.0024112	.255674
17	119.7	531.2	250	4.4377610	.0026770	.3042469
18	119.6	531.0	250	4.439799	.0022190	.3042469
19	118.8	527.2	280	4.4377106	.0026884	.3407566
20	118.8	527.4	280	4.439393	.00231013	.3407566
21	117.7	522.4	310	4.4384027	.0025328	.3772662
22	117.8	522.4	310	4.4346349	.0033796	.3772662
23	120.2	532.6	345	4.4309484	.00920814	.4198608

For Figure 3. Continued

SR. NO.	Frequency From Big Wheel N_B (C/S)	Frequency From Small Wheel N_S (C/S)	Longitudinal Strain Gauge Reading (μin/in)	N_S/N_B	Longitudinal Creep	Longitudinal Coefficient of Friction
24	120.1	533.1	345	4.4351081	.00327330	.4198608
25	120.3	533.4	345	4.433915	.0035414	.4198608
26	119.0	527.8	375	4.4352941	.00323151	.4563706
27	119.1	527.8	375	4.43157010	.00406842	.4563704
28	118.0	523.0	410	4.4322033	.003926107	.498965
29	118.1	522.8	410	4.4267569	.00515010	.498965
30	118.1	523.3	410	4.4309906	.00419864	.498965
31	117.2	516.8	440	4.40955631	.00901571	.5356746
32	117.4	515.7	440	4.3926746	.0128096	.5354746
33	117.6	516.7	440	4.3886054	.01372411	.5354746
			Slipping			

For Figure 4. Longitudinal Run

8" Wheel, Plain 1070, 36 RC - 332
Vertical Load - 748 lbs
Area of Contact - .019143 Sq. In.

SR NO.	Frequency From Big Wheel N_B (C/S)	Frequency From Small Wheel N_S (C/S)	Longitudinal Strain Gauge Reading (μ in/in)	N_S/N_B	Longitudinal Creep	Longitudinal Coefficient of Friction
1	125.3	557.4	25	4.4485235	.000258	.020256
2	125.2	557.3	25	4.44888	.00036	.020256
3	124.1	552.6	55	4.452860	.0007163	.044563
4	124.1	552.1	55	4.4488	.000189	.044563
5	121.8	541.9	105	4.44909	.0001295	.08508
6	121.9	542.0	105	4.4626	.0007654	.08508
7	119.9	533.4	155	4.4487	.002171	.12558
8	119.9	533.8	155	4.452043	.00053	.12558
9	120.0	533.4	155	4.445	.001050	.12558
10	118.0	524.9	210	4.4483	.00030	.17015
11	118.1	524.9	210	4.444538	.001153	.17015
12	118.2	525.6	210	4.4467	.000668	.17015
13	116.8	518.9	250	4.442636	.00158	.20256
14	116.7	518.5	250	4.443016	.00149	.20256
15	116.8	519.0	250	4.443673	.001388	.20256
16	121.2	537.8	300	4.437293	.002782	.24307
17	121.5	538.4	300	4.4312	.004135	.24307
18	121.2	538.6	300	4.44389	.001298	.24307
19	120.1	532.4	350	4.43297	.00375	.28358
20	119.9	532.4	350	4.440366	.00209	.28358
21	120.1	532.5	350	4.433805	.003566	.28358
22	118.2	524.6	405	4.43824	.0025694	.32814
23	118.2	524.5	405	4.43739	.002759	.32814

For Figure 4. Continued

SR NO.	Frequency From Big Wheel N_B (C/S)	Frequency From Small Wheel N_S (C/S)	Longitudinal Strain Gauge Reading (μ in/in)	N_S/N_B	Longitudinal Creep	Longitudinal Coefficient of Friction
24	116.7	517.5	450	4.43444	.00342	.36460
25	115.2	510.8	500	4.43402	.003516	.40512
26	115.1	510.6	500	4.43614	.00304	.40512
27	116.9	517.9	550	4.43028	.00435	.44563
28	117.0	518.7	550	4.43333	.003672	.44563
29	115.3	510.9	600	4.431069	.004185	.48614
30	115.4	510.6	615	4.43527	.00563	.49829
			Slip at 650			

For Figure 5. Longitudinal Run

8" Wheel, Plain 1070, 36 RC
Vertical Load - 988 165
Area of Contact - .0158147

SR NO.	Frequency From Big Wheel N_B (C/S)	Frequency From Small Wheel N_S (C/S)	Longitudinal Strain Gauge Reading (μ in/in)	N_S/N_B	Longitudinal Creep	Longitudinal Coefficient of Friction
1	123.7	550.4	30	4.44967	.000044	.018218
2	122.7	545.7	55	4.447632	.0005035	.0334001
3	122.7	545.8	55	4.448247	.00032	.0334001
4	120.6	536.5	90	4.44859	.0002633	.0546547
5	120.7	537.1	90	4.449875	.000045	.0546547
6	118.1	525.1	155	4.446232	.0007733	.0941275
7	117.8	523.9	155	4.447368	.0005179	.0941275
8	116.3	517.2	200	4.4471195	.0005739	.121549
9	116.5	517.5	255	4.44206	.00171	.154855
10	114.3	508.4	255	4.447944	.000388	.154855
11	112.7	501.2	300	4.447204	.0005547	.1821823
12	112.6	500.8	300	4.44760	.000465	.1821823
13	117.2	520.6	350	4.44197	.001729	.212546
14	117.2	520.7	350	4.442832	.001537	.212546
15	115.3	511.8	400	4.438855	.00243	.242909
16	115.3	512.6	400	4.44579	.000871	.242909
17	115.3	512.1	400	4.44145	.001846	.242909
18	113.7	505.3	450	4.4441512	.001240	.2732735
19	113.8	505.5	450	4.44200	.001723	.2732735
20	119.2	529.3	500	4.44043	.0020	.3036372
21	119.2	528.9	500	4.43708	.00283	.3036372
22	117.7	522.4	550	4.4384	.00253	.334001
23	116.3	514.9	600	4.427343	.0050211	.364364

For Figure 5. Continued

SR NO.	Frequency From Big Wheel N_B (C/S)	Frequency From Small Wheel N_S (C/S)	Longitudinal Strain Gauge Reading (μ in/in)	N_S/N_B	Longitudinal Creep	Longitudinal Coefficient of Friction
24	116.5	516.2	600	4.43090	0.00422	.364364
25	114.5	507.4	650	4.431441	.0041002	.3947284
26	113.3	502.0	700	4.4307149	.0042633	.4250921
27	111.4	493.9	750	4.41290843	.004627	.4554559

Loaded to Full Capacity

For Figure 23. Normal Load = 548 lbs

Coefficient of Friction	Actual Area A_{actual}	Theoretical Area A_{theor}	$\frac{A_{actual}}{A_{theor}}$
For 2000 Rev.			
0.15	.0047	.00466	1.0085
0.30	.0094	.00466	2.017
0.40	.0124	.00466	2.660
0.46	.0135	.00466	2.896
For 4000 Rev.			
0.15	.0070	.00466	1.5021
0.30	.0114	.00466	2.4463
0.40	.0143	.00466	3.0686
0.46	.0147	.00466	3.1545
For 6000 Rev.			
0.15	.0094	.00466	2.0171
0.30	.0134	.00466	2.8755
0.40	.0158	.00466	2.8755
0.46	.0158	.00466	3.3905
For 8000 Rev.			
0.15	.0112	.00466	2.4034
0.30	.0150	.00466	3.2188
0.40	.0169	.00466	3.6266
0.46	.0168	.00466	3.6051
For 10,000 Rev.			
0.15	.0123	.00466	2.6394
0.30	.0160	.00466	3.4334
0.40	.0175	.00466	3.7553
0.46	.0172	.00466	3.6909

For Figure 24. Normal Load = 748 lbs

Coefficient of Friction	Actual Area A_{actual}	Theoretical Area A_{theor}	$\frac{A_{actual}}{A_{theor}}$
For 2000 Rev.			
0.15	.0058	.00472	1.0139
0.30	.0120	.00572	2.0979
0.40	.0126	.00572	2.2027
0.46	.0132	.00572	2.3076
For 4000 Rev.			
0.15	.0084	.00572	1.4685
0.30	.0147	.00572	2.5699
0.40	.0150	.00572	2.6223
0.46	.0156	.00572	2.7272
For 6000 Rev.			
0.15	.0105	.00572	1.8356
0.30	.0167	.00572	2.9195
0.40	.0170	.00572	2.9720
0.46	.0174	.00572	3.0419
For 8000 Rev.			
0.15	.0121	.00572	2.1153
0.30	.0180	.00572	3.1468
0.40	.0184	.00572	3.2167
0.46	.0184	.00572	3.2167
For 10,000 Rev.			
0.15	.0134	.00572	2.3426
0.30	.0189	.00572	3.3041
0.40	.0190	.00572	3.3216
0.46	.0185	.00572	3.2342

For Figure 25. For Coefficient of Friction = 0.15

Load in Pounds	Experimental Area in Square In.
For 2000 Rev.	
548	0.0047
748	0.0058
1000	0.010
For 4000 Rev.	
548	0.0070
748	0.0084
1000	0.0115
For 6000 Rev.	
548	0.0094
748	0.0105
1000	0.0129
For 8000 Rev.	
548	0.0122
748	0.0121
1000	0.0139
For 10,000 Rev.	
548	0.0123
748	0.0134
1000	0.0146

For Figure 26. For Coefficient of Friction = 0.30

Load in Pounds	Experimental Area of Contact in square inches
For 2000 Rev.	
548	0.0094
748	0.0120
1000	0.0140
For 4000 Rev.	
548	0.0114
748	0.0147
1000	0.0162
For 6000 Rev.	
548	0.0134
748	0.0167
1000	0.0178
For 8000 Rev.	
548	0.0150
748	0.0180
1000	0.0188
For 10,000 Rev.	
548	0.0160
748	0.0189
1000	0.0194

Normal Load - 548 lbs

Longitudinal Coefficient of Friction - 0.15

8" Wheel, Plain 1070, 36 RC

SR NO.	Time of Run (minutes)	Longitudinal Creep	Area of Contact (square in.)	Area of Contact x Creep
1	60	.0012327	.004983	.0000061
2	120	.0009724	.01008	.0000098
3	180	.000819	.01107	.0000090
4	260	.0006633	.01283	.0000085
5	300	.0006138	.01385	.0000085

Normal Load - 548 lbs

Longitudinal Coefficient of Friction = 0.30

8" Wheel, Plain 1070, 36 RC

SR NO.	Time of Run (minutes)	Longitudinal Creep	Area of Contact (square in)	Area of Contact x Creep
1	45	.0020281	.00948	.0000192
2	90	.0017041	.01142	.0000194
3	135	.0015488	.01360	.0000210
4	165	.0014977	.01352	.0000202
5	210	.0013614	.01596	.0000217
6	270	.0013299	.01634	.0000217

Normal Load - 548 lbs

Longitudinal Coefficient of Friction - 0.40

8" Wheel, Plain 1070, 36 RC

SR NO.	Time of Run (minutes)	Longitudinal Creep	Area of Contact (square in.)	Area of Contact x Creep
1	30	.002919	.01210	.0000353
2	75	.0025971	.01360	.0000353
3	120	.0023936	.01524	.0000364
4	165	.00217	.01644	.0000356
5	210	.0020392	.01731	.0000352

Normal Load - 548 lbs
Longitudinal Coefficient of Friction - 0.46
8" Wheel, Plain 1070, 36 RC

SR. NO.	Time of Run (minutes)	Longitudinal Creep	Area of Contact (square in.)	Area of Contact x Creep
1	30	.003985	.01300	.0000518
2	90	.0035625	.01457	.0000519
3	150	.0032347	.01512	.0000489
4	180	.0031969	.01652	.0000528
5	240	.0030667	.01715	.0000522

Normal Load - 748 lbs

Longitudinal Coefficient of Friction - 0.15

8" Wheel, Plain 1070, 36 RC

SR NO.	Time of Run (munites)	Longitudinal Creep	Area of Contact (square in.)	Area of Contact x Creep
1	45	.0013794	.00581	.0000080
2	90	.0010447	.00866	.0000090
3	135	.0008274	.01083	.000089
4	180	.00071	.011659	.000082
5	225	.000618	.01365	.0000084
6	270	.0005811	.01516	.000088

Normal Load - 748 lbs

Longitudinal Coefficient of Friction - 0.30

8" Wheel, Plain 1070, 36 RC

SR NO.	Time of Run (minutes)	Longitudinal Creep	Area of Contact (square in.)	Area of Contact x Creep
1	45	.0023853	.01187	.0000283
2	90	.0019832	.01486	.0000235
3	135	.001762	.01624	.0000286
4	180	.0017092	.01764	.0000301
5	225	.0016478	.01867	.0000307
6	270	.0015228	.02031	.0000309

Normal Load - 748 lbs

Longitudinal Coefficient of Friction - 0.40

8" Wheel, Plain 1070, 36 RC

SR NO.	Time of Run (minutes)	Longitudinal Creep	Area of Contact (square in.)	Area of Contact x Creep
1	60	.0032905	.01326	.0000436
2	120	.0025723	.01610	.0000414
3	180	.0023146	.0177	.0000411
4	260	.00215	.01932	.0000415

Normal Load - 748 lbs

Longitudinal Coefficient of Friction - .46

8" Wheel, Plain 1070, 36 RC

SR NO.	Time of Run (minutes)	Longitudinal Creep	Area of Contact (square in.)	Area of Contact x Creep
1	45	.0041435	.01399	.0000579
2	135	.0033893	.01631	.0000573
3	165	.0033581	.01786	.0000599
4	210	.0032448	.01797	.0000583
5	255	.0032219	.01859	.0000598

Normal Load - 1000 lbs

Longitudinal Coefficient of Friction - 0.15

8" Wheel, Plain 1070, 36 RC

SR NO.	Time of Run (minutes)	Longitudinal Creep	Area of Contact (square in.)	Area of Contact x Creep
1	45	.0012543	.01071	.0000134
2	90	.0011552	.01221	.0000161
3	135	.0008424	.01267	.0000106
4	180	.0008061	.01368	.0000110
5	225	.0008262	.01476	.0000121
6	270	.0007972	.01478	.0000117

Normal Load - 1000 lbs

Longitudinal Coefficient of Friction - 0.30

8" Wheel, Plain 1070, 36 RC

SR NO.	Time of Run (minutes)	Longitudinal Creep	Area of Contact (square in.)	Area of Contact x Creep
1	45	.0026227	.01410	.0000369
2	90	.0022636	.01605	.0000363
3	135	.0021143	.01721	.0000363
4	180	.0019963	.01864	.0000372
5	225	.0019703	.01899	.0000374
6	270	.0019414	.02006	.0000389

BIBLIOGRAPHY

1. Itami, G.A., "The Study of Friction-Creep Phenomenon of Adhesion Between Steel Wheels and Rails", Thesis, General Motors Institute, 1968.

2. Karamchandani, K.C., S. Kumar, C.A. Sciammarella, B. Seth, L. Nialescu, and S. Kalpakjian, "Friction Creep and Wear Studies for Steel Wheels and Rails", May 1975.

3. Nayak, R.R., S. Hariharan, R. Stern, R. Abilock, P.A. March and P.K. Gupta, "Friction and Creep in Rolling Contact", Report No. RPA-RT-71-64, DOT, 1971.

4. Timoshenko, S., and J.N. Goodier, Theory of Elasticity, McGraw-Hill Book Company, Inc., New York, 1951.

5. Verbeeck, H., "Present Knowledge of Adhesion and Its Utilization", Rail International, 697-735, June 1973.

6. Kalker, J.J., "On the Rolling Contact of Two Elastic Bodies in the Presence of Dry Friction", Ph.D. Thesis, 1967.

7. Andrews, H.I., "The CREEP of Locomotive Driving Wheels, (Part I)", Rail Engineering International, January 1975.

8. Timoshenko, S., Strength of Materials, Part II, Advanced Theory and Problems, D. Van Nostrand Company, Inc., New York, 1940.

9. Andrews, H.I., "The CREEP of Locomotive Driving Wheels (Part I and II)", Rail Engineering International, January 1975.

10. Carter, F.W., "On the Action of a Locomotive Driving Wheel", Proc. Roy. Soc. A, Vol. 112, p. 151-157, 1926.

11. Poritsky, H., "Stresses and Deflections of Cylindrical Bodies in Contact with Application to Contact of Gears and Locomotive Wheels", Journal of Applied Mechanics, Trans, ASME, 72, 191-201, 1930.

Study of Friction and Creep Between Steel Wheels and Rail, 1976
US DOT, FRA, C Sciammarella, M Press, S Kumar, B Seth, S Naiescu, S Kalpakjian

U.S. DEPARTMENT OF TRANSPORTATION
FEDERAL RAILROAD ADMINISTRATION
Washington, D.C. 20590

Official Business

PENALTY FOR PRIVATE USE, $300

POSTAGE AND FEES PAID
FEDERAL RAILROAD
ADMINISTRATION
DOT 516

U.S. MAIL